[UCI]I804:24011-200000265226

2016 년 2 월

박사학위 논문

The Role of Sestrin2 in Metabolic Stress

조선대학교 대학원

약 학 과

서 규 화

The Role of Sestrin2 in Metabolic Stress

Sestrin2 에 의한 에너지 대사 스트레스 조절기전 연구

2016 년 2 월 25 일

조선대학교 대학원

약 학 과

서 규 화

The Role of Sestrin2 in Metabolic Stress

지도교수 신 상 미

이 논문을 약학 박사학위신청 논문으로 제출함

2015 년 10 월

조선대학교 대학원

약 학 과

서 규 화

서규화의 박사학위논문을 인준함

위원장 조선대학교 교수 최홍석 인

위 원 목포대학교 교수 박은영 인

위 원 조선대학교 교수 기성환 인

위 원 조선대학교 교수 이금화 인

위 원 조선대학교 교수 신상미 인

2015 년 12 월

조선대학교 대학원

CONTENTS

LIST OF FIGURES

Part I: Protection of mitochondrial function by Sestrin2 in glucose deprivation-induced cytotoxicity

Part II: Sestrin2 inhibits HIF-1α accumulation through increase of PHD activity and H_2O_2-scavenging effect

ABBREVIATIONS

ACC	Acetyl-coenzyme A carboxylase
5-FU	5-Fluorouracil
AICAR	5-Aminoimidazole-4-carboxamide-1-β-d-ribofuranoside
AMPK	AMP-activated protein kinase
ARE	Antioxidant response elements
CA-IX	Carbonic anhydrase-IX
CHX	Cycloheximide
DCFH-DA	2',7'-Dichlorofluorescein diacetate
DMOG	Dimethyloxalylglycine
DMSO	Dimethylsulfoxide
DN-AMPK	Dominant negative mutant of AMPK
EMT	Epithelial-mesenchymal transition
FoxO	Forkhead transcription factors
GLUT1	Glucose transporter 1
GSH	Glutathione
GSK3β	Glycogen synthase kinase 3β
H_2O_2	Hydrogen peroxide
HIF	Hypoxia-inducible transcription factor
HO-1	Heme oxygenase-1
HRE	Hypoxia response element
IB	Immunoblot

IP	Immunoprecipitation
LDH A	Lactate dehydrogenase A
mtCOX II	Mitochondrial cytochrome *c* oxidase subunit II
mtDNA	Mitochondrial DNA
mTOR	Mammalian target of rapamycin
mTORC	mTOR complex
MTT	3-(4,5-Dimethylthiazol-2-yl)-2,5-diphenyl-tetrazolium bromide
NAC	*N*-acetyl-L-cysteine
Nrf2	NF-E2-related factor 2
OH-HIF-1α	Hydroxyl-HIF-1α
OXPHOS	Oxidative phosphorylation
PDK1	Pyruvate dehydrogenase kinase 1
PHD	Prolyl hydroxylase domain
PRX	Peroxiredoxin
RIP140	Nuclear-encoded receptor-interacting protein 140
ROS	Reactive oxygen species
SESN	Sestrin
SOD	Superoxide dismutase
Ubi	Ubiquitin
VEGF	Vascular endothelial growth factor
VHL	von Hippel-Lindau

국 문 초 록

Sestrin2 에 의한 에너지 대사 스트레스 조절기전 연구

서 규 화

지 도 교 수: 신 상 미

약학과

조선대학교 대학원

세포는 정상적인 성장과 증식을 위해 기본 에너지 단위로 ATP 를 생성하여 활용한다. 미토콘드리아는 ATP 생성을 담당하는 세포내 소기관으로, 영양분과 산소를 이용해 세포가 필요로 하는 ATP 를 공급한다. 따라서 세포가 적절한 영양분과 산소를 공급받는 것은 미토콘드리아의 기능 유지에 필수적으로 요구된다. 그러나 이를 충족시키지 못할 경우, 세포는 ATP 생성이 감소되어 에너지 대사 스트레스에 노출된다. 대사 스트레스는 미토콘드리아 전자전달계의 정상적 기능을 방해하여, 활성 산소종 (reactive oxygen species, ROS)을 발생시키고, 세포는 변질된 신호를 생성하게 된다. 세포는 이러한 활성산소에 의한 산화적 스트레스 (oxidative stress)를 방어하기 위해 정상범위의 활성산소를 유지할 수 있는 항산화 시스템을 갖추고 있다.

신규 항산화 분자인 Sestrin2 (SESN2)는 산화적 스트레스를 포함한 다양한 자극에 의해 발현이 증가되어, 활성산소종을 감소시킨다. SESN2 의 이러한 기능은 세포내 항산화 단백질인 peroxiredoxin 의 재활성을 돕는 과정에서 기인한다. 본 연구는 항산화 분자로 보고된 SESN2 이 영양분과 산소가 결핍된 대사 스트레스에서 어떠한 역할을 담당하는지 평가하고, 이 과정에 매개되는 세포 내 신호 전달과정을 규명하고자 하였다.

첫 번째 연구에서는 포도당 결핍에 따른 대사 스트레스에서 SESN2 의 역할을 규명하였다. 절식시킨 마우스에서 분리한 간세포의 SESN2 단백질 양은 정상 식이 마우스의 간세포에 비해 증가되어 있었다. 또한 세 가지 간세포 (AML12, Huh7, HepG2) 모델에서도 포도당 결핍 시 SESN2 의 발현이 증가됨을 확인할 수 있었다. 반면, 정상 범위보다 높은 포도당 공급 시, SESN2 의 발현 수준은 변화하지 않았다. HepG2 세포에서 포도당 고갈로 인한 SESN2 의 mRNA 발현 증가와 SESN2 의 luciferase 활성 증가를 확인하였다. 또한 SESN2 의 유도가 전사적 조절 기전에 기인함을 포도당 고갈로 인한 Nrf2 인산화 증가를 통해 확인하였다. 다음으로 증가된 SESN2 의 기능적 역할을 평가하기 위해, SESN2 과발현 세포주를 만들어 포도당을 고갈 시킨 후 미토콘드리아 기능 변화를 관찰하였다. 포도당 고갈은 ADP/ATP ratio 를 증가시켰고, 그리고 미토콘드리아 막전위와 DNA 수치를 현저하게 감소시켰다. 그렇지만, SESN2 과발현 세포주에서는 포도당 고갈로 증가한 ADP/ATP ratio 가 억제 되었고, 미토콘드리아 막전위와 DNA 수치를 회복시켰다. 더 나아가 SESN2 과발현 세포주는 포도당 고갈로 인한 세포 사멸을 현저하게 억제시켰다. 에너지 고갈 스트레스에서 SESN2 의 미토콘드리아 기능 회복과 세포

사멸 억제 효능을 신호 전달 경로 측면에서 확인하기 위해, 세포 내 에너지 신호인 AMPK 의 활성을 조사하였다. SESN2 과발현 세포주에 AMPK 불활성형인 DN-AMPK 를 형질전환 시킨 결과, SESN2 과발현에 의해 회복된 미토콘드리아 막전위는 다시 감소하였다. 반면, AMPK 활성화제인 AICAR 의 사용은 포도당 고갈 상태에서 감소한 세포 생존률을 증가시켰다. 이러한 결과들은 SESN2 의 포도당 고갈에 따른 미토콘드리아 손상과 세포 사멸 방어 효능에 AMPK 활성이 동반되어야 함을 시사한다. 종합적으로 본 연구를 통하여 에너지 결핍 상태에서 SESN2 가 미토콘드리아 기능 회복 및 세포 생존에 기여하였고, 여기에는 AMPK 활성이 동반됨을 확인하였다.

두 번째 연구에서는 SESN2 가 산소가 결핍된 상황에서 변질되는 신호들을 억제하는 기전을 규명하였다. Hypoxia-inducible transcription factor-1α (HIF-1α)는 저산소 상태에서 축적되는 단백질로 세포의 적응 반응을 유도하여 암의 성장 및 이동을 촉진하는 주요한 전사인자이다. 이러한 사실을 바탕으로, SESN2 이 HIF-1α의 조절을 통해 암세포에서 특이적으로 변질된 기능을 억제하는지 살펴보고자 하였다. 사람의 대장암 세포주 (HCT116 과 HT29)를 저산소증 상태 또는 $CoCl_2$ 에 노출 시 HIF-1α의 단백질 증가를 관찰할 수 있었다. 이 때, SESN2 를 외인적으로 과발현시킨 결과 누적된 HIF-1α을 유의성 있게 감소시켰다. 또한 SESN2 과발현 세포는 $CoCl_2$ 로 유도된 hypoxia response element (HRE) luciferase 활성을 억제시켰으며, HIF-1α 의 타겟 유전자의 발현 증가도 유의적으로 감소시켰다. 이러한 SESN2 에 의한 HIF-1α 억제의 기능적 지표를 평가하고자 암세포의 이동 및 침습성을 관찰하였다. 혈청 자극으로 유도된 암세포의 이동 및 침습성이 SESN2 과발현

세포에서 효과적으로 억제되었다. 다음으로 SESN2 에 의한 HIF-1α 억제 기전을 규명하고자, HIF-1α mRNA 수준을 관찰하였다. SESN2 과발현은 HIF-1α mRNA 발현에 영향을 끼치지 않았고, 이를 기초로 SESN2 가 mRNA 전사과정 이후의 단계를 조절하는 것으로 가정할 수 있었다. 이에, SESN2 가 HIF-1α의 단백질 분해 단계에 미치는 영향을 평가하고자 하였다. Cycloheximide (단백질 번역 억제제)과 $CoCl_2$ 를 병용처리하여 HIF-1α의 분해과정을 시간별로 관찰한 결과, SESN2 과발현 세포는 더 큰 폭으로 단백질이 분해되는 결과를 나타냈다. 또한, SESN2 과발현 세포는 HIF-1α의 ubiquitination 을 더욱 증가시켰으며, ubiquitination 이 되기 위해 일어나는 HIF-1α의 수산화 역시 현저하게 증가시켰다. 이는 SESN2 가 HIF-1α의 분해를 가속화시킴을 시사한다. SESN2 의 하위 신호로 규명된 AMPK 가 이러한 효능에 관여하는지 알아보고자 SESN2 과발현 세포주에 siRNA 를 이용하여 AMPK 의 발현을 억제하였다. 그 결과, SESN2 에 의해 감소되었던 HIF-1α 단백질 수준이 다시 증가되었고, HIF-1α 수산화는 억제되었다. 또한, AMPK 불활성형인 DN-AMPK 를 형질 전환 도입한 결과, SESN2 에 의한 HIF-1α 축적 억제가 반전됨을 확인하였다. 더 나아가 SESN2–AMPK 활성화로 증가된 HIF-1α 수산화가 세포의 이동 및 침습성에도 억제효능을 나타낼 수 있는 지 확인하기 위해 prolyl hydroxylase (PHD, HIF-1α 수산화화 가능 효소) 억제제인 dimethyloxalylglycine (DMOG)를 도입하였다. DMOG 는 SESN2 에 의한 HIF-1α 억제 및 HIF-1α 수산화 증가 효과를 유의적으로 반전시켰다. 더 나아가 SESN2 에 의해 억제된 암세포의 이동 및 침습성이 DMOG 처리상태에서 다시 회복됨을 확인하였다. 이러한 결과들은 SESN2 가 하위 AMPK 를 매개로 하여 HIF-1α의 수산화를 증가시키고,

이는 HIF-1α의 분해 촉진을 유도하여 암세포의 이동성을 억제할 수 있음을 의미한다.

종합적으로, 본 연구에서는 에너지 대사 스트레스에서 신규 항산화 단백질인 SESN2 의 역할을 규명하였다. 에너지 대사 스트레스에서 SESN2 의 세포 소기관 보호 및 세포 보호, 그리고 저산소증 적응 반응 억제를 통한 암세포 이동 및 침습 억제 효능을 규명함으로써 에너지 대사 스트레스로 야기되는 병리과정을 교정할 수 있는 신규 타겟으로 SESN2 의 가능성을 제시하였다.

I. INTRODUCTION

1. Oxidative stress

1.1. Reactive oxygen species (ROS)

ROS are the chemical molecules that are formed upon incomplete oxygen reduction (D'Autréaux and Toledano, 2007; Drummond et al, 2011). In cells, ROS including superoxide anion, hydrogen peroxide and hydroxyl radical can be produced by normal cellular processes (Sies, 2014). The major sources of intracellular ROS are the mitochondrial electron transport chain and NADPH oxidases (D'Autréaux and Toledano, 2007; Drummond et al, 2011; Lemasters and Nieminen, 1997). These ROS are involved in signaling pathways of growth factors, cytokines, and hormones (D'Autréaux and Toledano, 2007; Drummond et al, 2011). Therefore, the role of ROS in cell proliferation and differentiation has been widely documented (Finkel, 2003; Martindale and Holbrook, 2002). However, uncontrolled ROS are involved in the cellular toxicity because of their greater chemical reactivity with cellular components (Imlay, 2003). Oxidative stress can be defined as an imbalance between prooxidants and antioxidants leading to a disruption of redox system (Finkel, 2003; Jones, 2008). Excessive ROS are subsequently converted into a number of more reactive derivatives like reactive nitrogen species (RNS), which induces detrimental effects on the cells (Brown and Borutaite, 2001). This oxidative stress leads to the damage of proteins, lipids, and DNA (Blumberg, 2004; D'Autréaux and Toledano, 2007). Thus, redox systems in cells are required to neutralize ROS and to maintain proper cellular function.

1.2. Cellular redox system

Cellular redox system can activate several genes to modulate ROS level, which contributes to prevent cellular damage (Martindale and Holbrook, 2002; Valko et al, 2006; 2007). The antioxidant enzymes such as superoxide dismutases (SODs), catalase, glutathione (GSH), thioredoxins (TRXs) and peroxiredoxins (PRXs) are distributed in cells and they are essential for maintaining the relevant concentration of ROS (Handy and Loscalzo, 2012). SODs convert superoxide radical to O_2 and H_2O_2 (Forman and Fridovich, 1973). Further oxygen metabolite, H_2O_2 is converted to O_2 and H_2O with the help of catalase (Deisseroth and Dounce, 1970). In addition, the most abundant low molecular-weight thiol-containing protein, GSH plays a major function in the control of H_2O_2 (Go and Jones, 2010). TRX is a key antioxidant protein regulating protein dithiol/disulfide balance by its disulfide reductase activity (Argyrou and Blanchard, 2004). The reaction mechanism is involved in the reduction of the enzyme active site cysteine sulfinic acid to thiol and electron transfer from the thiol to H_2O_2 (Argyrou and Blanchard, 2004). Another antioxidant protein, PRXs reduce mitochondrial and cytosolic H_2O_2 (Go and Jones, 2010; Lim et al, 2008; Noh et al, 2009; Rhee et al, 2003). To combat excessive ROS, antioxidant proteins exist in cells and they can defend the cells against oxidative stress.

2. Mitochondria

2.1. Mitochondrial function

Mitochondria are the powerhouses in cells because they are responsible for energy production. Cells enable to utilize the value of nutrients in the form of ATP by mitochondria (Green and Reed, 1998; Kroemer and Reed, 2000). Mitochondria have the processes of respiration and oxidative phosphorylation (OXPHOS), which produces cellular energy from glucose and oxygen (Jones, 1986). However, in this course, mitochondrial respiratory chain can produce ROS (Cadenas and Davies, 2000; Yu et al, 2006). Especially, it is a major intracellular source of ROS generation during pathological condition (DiMauro and Schon, 2003; Rolo and Palmeira, 2006; Yu et al, 2006). Excessive ROS generation causes changes of mitochondrial membrane permeability, which is indicative of mitochondrial dysfunction (Lemasters et al, 1998). Loss of outer and inner mitochondrial membranes permeability subsequently triggers an event of cell death, either by apoptosis or by necrosis (Green and Reed, 1998). Therefore, maintenance of mitochondrial membrane permeability is important in cell metabolism and injury.

2.2. Role of the mitochondria in apoptosis

Mitochondria are important organelle for initiation of apoptosis signal cascade (Kadenbach and Hüttemann, 2015; Kim et al, 2003; Wang, 2001). Mitochondrial damage can cause disruption of electron transport chain and ATP production, and activation of caspase family, finally promotes cell death (Kim et al, 2003; Lemasters et al, 1998). Loss of mitochondrial membrane potential and the subsequently release of cytochrome *c* starts the apoptotic signal pathway (Green and Reed, 1998; Hunter et al, 1976; Kadenbach and Hüttemann, 2015; Kroemer and Reed, 2000; Petronilli et al, 2001). The outer membrane of

mitochondria is broken as a result of the mitochondrial matrix swelling, which allows cytochrome *c* to escape from mitochondria (Green and Reed, 1998). Release of cytochrome *c* from the mitochondria can provoke a series of events leading to the activation of caspase-9, a cysteine protease (Green and Reed, 1998; Kroemer and Reed, 2000; Petronilli et al, 2001). Caspase-9 activates effector caspase-3, which can cause cleavage of PARP (Brown and Borutaite, 2001). Cleaved PARP facilitates DNA fragment and ensures irreversibility of the apoptosis signal cascade (Brown and Borutaite, 2001). Hence, mitochondria are critical place in controlling cell survival and death.

3. Metabolic stress

3.1. Imbalance of nutrition

Metabolic stress is defined as alteration of intracellular glucose and oxygen balance, which induces modification of cell components and enhances the ROS production (Blackburn et al, 1999). Therefore, imbalance of diet is a direct cause of metabolic stress. Obesity is a serious hypernutritional problem, as it increases the risk of morbidity from several pathologies including hypertension, hyperlipidemia, type 2 diabetes, stroke, non-alcoholic fatty liver disease, and cancers (WHO, 2012). Many *in vivo* studies have shown that obesity is coupled with altered redox state and increased metabolic risk (Codoñer-Franch et al, 2012; Hermsdorff et al, 2012; Warolin et al, 2014). Chronic hypernutrition stimulates intracellular pathways leading to oxidative stress through multiple biochemical mechanisms, such as superoxide

generation from NADPH oxidases and OXPHOS (Serra et al, 2012; Sies et al, 2005). Moreover, oxidative stress also plays a critical role in the development of obesity by stimulating white adipose tissue deposition increases pre-adipocyte proliferation and adipocyte differentiation (Furukawa et al, 2004; Lee et al, 2009a).

Lack of proper glucose supply also represents metabolic stress accompanying the intracellular ATP depletion (Lee et al, 2010a). Decrease of mitochondrial ATP production can cause changes in membrane phospholipids and proteins (Scholte, 1988). In addition, ATP depletion redirects the death program towards apoptosis (Nicotera et al, 1998). Therefore, glucose deprivated-cells activate signal transduction pathways inducing the expression of a battery of stress responsive genes (Ahmad et al, 2005; Lee et al, 2010a). Ahmad et al. showed that depletion of glucose supply enhances representative markers of oxidative stress (Ahmad et al, 2005). Collectively, balanced supply of nutrition is essential for mitochondrial function and finally cell survival.

3.2. Imbalance of oxygen: hypoxia and HIF-1α regulation

Oxygen is necessary for cell proliferation, bacterial defense and recovery of wound (Kondo and Ishida, 2010). Most importantly, oxygen is the essential ingredient for making energy in a process called cellular respiration (Gnaiger et al, 2000). It enables electron transfer in mitochondrial respiratory chain, which plays a major role in ATP production (Gnaiger et al, 2000). Therefore, when environment of cell is changed to hypoxia (low level of oxygen), cells alter their transcriptional profiles to modulate glycolysis, proliferation, and survival against hypoxic stress (Giaccia et al, 2003). The hypoxia-inducible transcription factor-1α (HIF-1α) is a primary transcription factor in hypoxia-adaptive response (Giaccia et al, 2003; Ke and Costa,

2006; Lee et al, 2009b). HIF-1α is unstable in well-oxygenated condition owing to ubiquitin-mediated degradation, but rapidly becomes stable in hypoxic conditions (Giaccia et al, 2003). Degradation is mediated via hydroxylation of prolines 402 and 564 of HIF-1α by prolyl hydroxylases (PHDs) (Giaccia et al, 2003; Jaakkola et al, 2001; Lum et al, 2007). The hydroxylated prolines are recognized by VHL, targeting the HIF-1α subunits for degradation (Gossage et al, 2015). However, PHDs activity is limited by hypoxia, so HIF-1α hydroxylation is blocked and finally HIF-1α is stabilized (Kaelin Jr, 2008; Keith et al, 2012). The stabilized HIF-1α pairs with HIF-1β (also known as aryl hydrocarbon receptor nuclear translocator, ARNT) and then translocates to the nucleus and binds to hypoxia response elements (HREs) to induce HIF-1α-dependent gene transcription (Giaccia et al, 2003; Lee et al, 2009b). Because tumor cells are easily exposed to hypoxic condition, HIF-1α is activated and overexpressed in various cancers (Borren et al, 2013; Giaccia et al, 2003; Qin et al, 2015; Yang et al, 2008). This finding has indicated that HIF-1α-signaling pathway is a crucial to regulate metabolism and growth in tumor.

4. Sestrin2 (SESN2)

4.1. Discovery of SESNs: an emerging family of stress response protein

SESNs are highly conserved stress-responsive proteins and three isoforms were reported (Budanov et al, 2010; Lee et al, 2013). SESN1 and SESN2 were identified as p53 target genes, their expression were implicated in defense mechanism against oxidative stress and genotoxic

stress (Budanov et al, 2002; 2010; Budanov and Karin, 2008). SESN1, also known as p53-activated gene 26 (PA26), is a potential regulator of cellular growth (Buckbinder et al, 1994; Velasco-Miguel, 1999). Hypoxia induced gene 95 (Hi95), better known as SESN2, plays a crucial role in cytoprotection under oxidative stress (Budanov et al, 2002; Shin et al, 2012). More recently, NF-E2-related factor 2 (Nrf2)-antioxidant response elements (ARE) pathway which regulates expression of antioxidant genes was found to control SESN2 gene induction (Shin et al, 2012). A third member of SESNs family, SESN3, has been reported to induce SESN1 (Nogueira et al, 2008; Tran et al, 2002) and is regulated by serum and growth factors (Budanov et al, 2002; Peeters et al, 2003). In comparison to p53 dependent induction of SESN1 and SESN2, SESN3 is activated by forkhead transcription factors (FoxO) (Nogueira et al, 2008).

4.2. Role of the SESN2 in redox homeostasis

The mammalian PRX family consists of six members, which control hydrogen peroxide concentration under oxidative stress (Chang et al, 2004; Lim et al, 2008). During oxidative stress, the PRXs can be over-oxidized to cysteine sulfinic acid, resulting in their inactivation (Rhee et al, 2003). In oxidized form of PRXs can be rescued by a special sulfinylreductase system comprised of sulphiredoxins (Biteau et al, 2003; Chang et al, 2004). SESN2 can restore the activity of over-oxidized PRXs in cells (Budanov et al, 2004; Essler et al, 2009; Lee et al, 2013). Knockdown of SESN2 in cultured cells results in ROS accumulation, whereas SESN2 overexpression reduces cellular ROS levels (Budanov et al, 2004). Shin et al. showed that SESN2 can protect cells from oxidative stress (Shin et al, 2012). In addition, SESN2 appeared to be protective against energetic stress-induced apoptosis that result in integrate pro-survival

factor (Ben-Sahra et al, 2013).

4.3. SESN2 and cellular signaling

SESN2 controls metabolic adaptation of cells in response to diverse stress by regulation of the AMP-activated protein kinase (AMPK)-mammalian target of rapamycin (mTOR) signaling axis (Budanov and Karin, 2008; Sanli et al, 2012). AMPK and mTOR are crucial nutrient-sensing protein kinases and each has antagonistic functions in metabolic homeostasis (Hardie et al, 2012; Zoncu et al, 2011). AMPK phosphorylates various enzymes, such as acetyl-coenzyme A carboxylase (ACC) and glycogen synthase, directly suppresses their enzymatic activities in glycogen and lipid biosynthesis (Hardie et al, 2012). Importantly, AMPK can directly inhibit mTOR complex 1 (mTORC1) through phosphorylation-dependent inhibition of regulatory subunit raptor (Gwinn et al, 2008). SESN2 induces phosphorylation of AMPK and enhances AMPK-mediated phosphorylation of the TSC1:TSC2 complex (Budanov and Karin, 2008). In addition, overexpression of SESN2 in cells results in strong inhibition of mTORC1 activity (Budanov and Karin, 2008). Importantly, hepatosteatosis in SESN2-knockout mice can be corrected by restoration of AMPK activity (Lee et al, 2012a), supporting that AMPK as a major mediator of SESN2 effects on metabolism. Collectively, these results show that SESN2 is a crucial regulator of cellular metabolism acting via the AMPK-mTORC signaling axis.

5. Implication of SESN2 in human diseases

5.1. Role of SESN2 in metabolic diseases

Accumulated reports supported that SESN2 has many beneficial effects in metabolic diseases (Bae et al, 2013; Eid et al, 2013; Jin et al, 2013; Lee et al, 2010b). Fasting and refeeding states regulate SESN2 level in mouse liver (Bae et al, 2013). Moreover, SESN2 decreases high glucose-induced dysfunction of endothelial nitric oxide synthase and synthesis of fibronectin in glomerular mesangial cells (Eid et al, 2013). In addition, SESN2 attenuates hepatic lipogenesis (Jin et al, 2013). Moreover, in *Drosophila*, SESN-null flies have increased lipid accumulation in the fat body, the *Drosophila* homologue of the mammalian liver, which is associated with reduced AMPK activity and enhanced TOR activity (Lee et al, 2010b). Importantly, feeding of SESN-null *Drosophila* larvae with rapamycin or the AMPK activator 5-aminoimidazole-4-carboxamide-1-β-d-ribofuranoside (AICAR) attenuates degenerative phenotypes observed in skeletal muscle (Lee et al, 2010b). Collectively, these reports indicate that SESN2 is responsively induced under metabolic stress in cells and can modulate cellular metabolism-related signaling. The present study further investigated that glucose deprivation-induced metabolic stress increased ROS production leading to the induction of SESN2, which protected mitochondrial damage and cell death. In addition, the pivotal role of SESN2–AMPK activation in adaptive survival response was examined.

5.2. Suppression of cancer cell growth and proliferation by SESN2

SESN2 inhibits cell growth and proliferation in many cancer cell lines including lung and breast carcinoma (Budanov et al, 2002; Budanov and Karin, 2008). SESN2 prevents translation of c-Myc and Cyclin D1 mRNAs, thus, suppresses cell proliferation (Budanov and

Karin, 2008). Moreover, SESN2 was originally isolated as a gene activated by hypoxia in human neuroblastoma cells (Budanov et al, 2002). In addition, lack of SESN2 mouse embryonic fibroblast was significantly more responsible to Ras-induced oncogenic transformation than wild type cells (Budanov and Karin, 2008). Silencing of SESN2 together with p53 accelerates lung cancer cell growth in a mouse tumor xenograft model (Sablina et al, 2005). Based on these previous reports that SESN2-dependent regulation of cell proliferation can be important during tumorigenesis, this study aimed to investigate the inhibitory role of SESN2 in cancer pathophysiology under hypoxia and its molecular mechanism.

II. STUDY AIMS

1. The first study investigated whether glucose deprivation causes ROS mediated mitochondria impairment and apoptosis, and if so, whether a novel antioxidant SESN2 protects cells from the mitochondrial dysfunction and apoptosis. Finally, this study examined the role of SESN2–AMPK in recovery of mitochondrial function and cytoprotection.
2. The second study investigated whether a novel antioxidant SESN2 inhibits HIF-1α and *in vitro* cell metastasis in colrectal cancer cells. Moreover, the role of SESN2–AMPK activation on regulation of HIF-1α degradation was studied.

III. MATERIALS AND METHODS

1. Materials

Anti-HIF-1α antibody was provided by BD Biosciences Pharmingen (San Jose, CA). Anti-SESN2 antibody and anti-HIF-1β antibody were purchased from Proteintech (Chicago, IL). Antibody against phospho-ACC, phospho-AMPK, AMPKα, caspase-3, hydroxyl-HIF-1α (proline 564) and ubiquitin were purchased from Cell Signaling Technology (Danvers, MA). Anti-Bcl-x_L antibody, anti-Nrf2 antibody, anti-PARP antibody and rhodamine 123 were obtained from Santa Cruz Biotechnology (Santa Cruz, CA). Mn-TBAP was purchased from Cayman Chemical (Ann Arbor, MI). Cycloheximide (CHX), cyclosporin A, dimethyloxalylglycine (DMOG), 5-fluorouracil (5-FU) and MG132 were purchased from Calbiochem (San Diego, CA). Phospho-Nrf2 antibody and PHD2 antibody were purchased from NOVUS Biologicals (Littleton, CO). Glucose-free Dulbecco's modified Eagle's medium (DMEM) was obtained from Life Technology (Gaithersburg, MD). Actinomycin D (Act D), AICAR, anti-β-actin antibody, PEG-catalase (catalase), cobalt chloride ($CoCl_2$), 2',7'-dichlorofluorescein diacetate (DCFH-DA), dimethylsulfoxide (DMSO), hydrogen peroxide (H_2O_2), 3-(4,5-dimethylthiazol-2-yl)-2,5-diphenyl-tetrazolium bromide (MTT), *N*-acetyl-L-cysteine (NAC), rotenone, trolox, and other reagents were purchased from Sigma Chemicals (St. Louis, MO).

2. Cell culture

A human hepatoma-derived cell line (HepG2), murine hepatocyte cell line (AML12) and human colorectal cancer cell lines (HCT116 and HT29) were obtained from the American Type Culture Collection (Manassas, VA). HepG2, HCT116 and HT29 cells were maintained in

DMEM and Huh7 (a human hepatoma-derived cell line) cells were maintained in RPMI. AML12 cells were cultured in 1:1 mixture of DMEM and Ham's F12 medium (Hyclone, Logan, UT) with insulin/transferrin/selenium solution (Life Technologies, Gaithersburg, MD) and 40 ng/ml dexamethasone (Sigma Chemicals St. Louis, MO). All cells were maintained in media with supplement of 10% fetal bovine serum (FBS; Hyclone, Logan, UT) and 50 units/mL penicillin/streptomycin. Cells were grown at 37°C in a humidified 5% CO_2 atmosphere. For experiments, cells were plated in plates for 2–3 days (i.e., reached around 80%) and medium removed and replaced with a fresh serum-free medium for overnight before treatments. To generate hypoxic condition, cells were maintained in either normoxic (21% O_2 and 5% CO_2) or hypoxic (1% O_2, 5% CO_2, and N_2 balance) conditions at 37^{o}C using a hypoxia incubator (Galaxy 48R, New Brunswick [Eppendorf], Hamburg, Germany).

3. Establishment of a stable cell line expressing SESN2

For preparation of stably expressing SESN2 cells, HepG2 cells were transfected with the plasmid pCMV-Tag3A (MOCK-transfected) or pCMV-SESN2 (geneticin-resistant SESN2 overexpressed) by using Lipofectamine 2000 (Invitrogen, Carlsbad, CA) following the manufacturer's protocol. One day after transfection, formation of colonies, which were geneticin-resistant, were selected by incubation with geneticin (500 μg/mL). Geneticin-resistant cells were grown and amplified in culture. Overexpression of SESN2 was confirmed by immunoblot analysis.

4. Recombinant adenovirus SESN2 constructs infection

The plasmid encoding a SESN2 was kindly provided by Dr. Il Je Cho (Deagu Haany

University, Daegu, Korea). HCT116 or HT29 cells were infected with adenovirus and incubated for 36 h, and then serum starved for 12 h. Then cells were treated with the indicated reagent. Ad-LacZ or Ad-GFP was used as an infection control. Efficiency of infection was consistently >90% with this method.

5. Primary hepatocyte isolation

All animal experiments were approved by the the guidelines of the Institutional Animal Use and Care Committee at Chosun University. Primary hepatocytes were isolated from male ICR mice (Samtako, Korea) as previously described (Jin et al, 2013). Briefly, the mouse was anesthetized with injection of Zoletil (Virbac, France) and portal vein was cannulated. Then, the liver was perfused by HBSS containing 0.1% collagenase and calcium. After the liver was collected, it was minced gently with scissors and suspended with DMEM. The cell suspension filtered through a cell strainer (70 μm), and then centrifuged at 400 rpm for 5 min to separate parenchymal and nonparenchymal cells. Isolated hepatocytes were plated on collagen-coated dishes and cultured in DMEM supplement of 10% FBS and 75 units/mL penicillin/streptomycin. Viability of isolated cells was determined via trypan blue staining; the viability of the isolated hepatocytes was usually 80–90%.

6. MTT assay

Cells were seeded in a 48-well plate. MTT was dissolved in PBS, and cells were incubated with the MTT solution for 3 h. Formation of formazan crystals was dissolved in DMSO. Absorbance at 570 nm was measured using a microplate reader (Spectramax 190, Molecular Device, Sunnyvale, CA). Cell viability was calculated relative to the untreated control according

to the following formula: cell viability (% control) = 100 × (absorbance of treated sample) / (absorbance of control).

7. Measurement of ROS generation

DCFH-DA, which is a nonpolar compound that is converted into polar derivative (dichlorofluorecein) by cellular esterase following incorporating in to cells (Métivier et al, 1998), was used to detect intracellular H_2O_2. The cells were seeded in 12-well plate and incubated under the indicated conditions. Cells were stained with 10 μM DCFH-DA during the final 1 h at 37°C. After all treatments, the cells were harvested by trypsinization and washed twice with PBS. Generation of hydrogen peroxide was measured using a fluorescence microplate reader (Gemini XPS, Molecular Device, Sunnyvale, CA) at excitation/emission wavelength of 485/525 nm. ROS production was normalized to the protein concentration and calculated relative to the vehicle-treated control according to the following formula: ROS production (fold of control) = [(relative fluorescence unit of treated sample)/(protein concentration of treated sample)] / [(relative fluorescence unit of vehicle-treated control)/(protein concentration of vehicle-treated control)].

8. Mitochondrial membrane permeability analysis

Changes in mitochondrial membrane permeability were calculated based on the rhodamine 123 uptake. Rhodamine 123, a membrane-permeable cationic fluorescent, binds to the mitochondrial membranes. Cells were stained with 0.05 μg/mL rhodamine 123 for last 1 h treatment. Sample collection and detection of fluorescence intensity were conducted as described in ROS production.

9. Immunoblot analysis

Whole cell lysates were prepared in ice-cold RIPA lysis buffer as described previously published procedures (Seo et al, 2014). Equal amount of protein samples were loaded in to a 7.5% or 12% SDS-gel, and blotted onto nitrocellulose membranes. After the membranes were blocked with 5% skim milk, they were immunostained with primary antibody overnight at 4°C and then incubated with horseradish peroxidase-conjugated a secondary antibody. Specific protein bands were visualized by incubating the membrane with an ECL chemiluminescence system (GE Healthcare, Buckinghamshire, UK). Immunoblotting for β-actin confirmed equal loading of proteins.

10. Immunoprecipitation assay

Whole cell lysates (1.5 mg) were incubated with anti-HIF-1α antibody overnight at 4°C with continuous mild agitation. After antibody-antigen reaction, the antigen-antibody complexes were precipitated following a short incubation with protein G-agarose at 4°C. The captured immunocomplexes were washed 3 times with RIPA buffer prior to the addition of 2X Laemmli buffer and heating at 100°C for 5 min. Samples were separated on SDS–PAGE and analyzed as immunoblotting.

11. RNA isolation and RT-PCR analysis

Total RNA was isolated using Trizol (Invitrogen, Carlsbad, CA) according to the protocol provided by the manufacturer. The RNA was then reverse transcribed using an oligo$(dT)_{16}$ primer. PCR was conducted using a PCR premix (Bioneer, Daejeon, Korea) and a Thermal

Cycler (T100, Bio-Rad, Hercules, CA). GAPDH confirmed equal loading of total mRNA. The following primer pairs were used for PCR: human SESN1 5'-CTTCTGGAGGCAGTTCAAGC-3 (forward) and 5 -TGAATGGCAGCCTGTCTTCAC-3 (reverse); human SESN2 5 -CTCACACCATTAAGCATGGAG-3 (forward) and 5 -CAAGCTCGGAATTAATGTGCC-3 (reverse); and human GAPDH 5 -GAAGATGGTGATGGGATTTC-3 (forward) and 5 -GAAGGTGAAGGTCGGAGTC-3 (reverse).

12. Real-time PCR analysis

Quantitative real-time PCR was performed with StepOne (Applied Biosystems, Foster City, CA) using a SYBR Green premix according to the manufacturer's instructions (Applied Biosystems, Foster City, CA). PCR was performed using primers selective for the genes encoding haman vascular endothelial growth factor (VEGF) 5 -AGGAGGGCAGAATCATCACG-3 (forward) and 5 -CAAGGCCCACAGGGATTTTCT-3 (reverse), glucose transporter 1 (GLUT1) 5 -TGACGATACCGGAGCCAATG-3 (forward) and 5 -CGGGCCAAGAGTGTGCTAAA-3 (reverse), carbonic anhydrase-IX (CA-IX) 5 -CTTGGAAGAAATCGCTGAGG-3 (forward) and 5 -TGGAAGTAGCGGCTGAAGTC-3 (reverse), lactate dehydrogenase A (LDH A) 5 -AGCCCGATTCCGTTACCT-3 (forward) and 5 -CACCAGCAACATTCATTCCA-3 (reverse), pyruvate dehydrogenase kinase 1 (PDK1) 5 -ACAAGGAGAGCTTCGGGGTGGATC-3 (forward) and 5 -CCACGTCGCAGTTTGGATTTATGC-3 (reverse).

13. Transient transfection and luciferase assay

Cells were seeded in 12-well or 6-well plates and grown for overnight. Next day, the

transfection complexes containing the human SESN2 reporter plasmid and pRL-TK control plasmid (encoding for *Renilla* luciferase) and either dominant negative mutant of AMPK (DN-AMPK) or pCDNA (control) with Lipofectamine reagent (Invitrogen, San Diego, CA) were added to each well (Hwahng et al, 2009). HRE-A549 cells had been stably transfected with a HRE reporter gene containing the luciferase gene downstream of HRE (Lee et al, 2009b). After adenovirus infection, HRE-A549 cells were transfected with pRL-TK control plasmid. After 3 h, the transfection complexes were removed and cells were incubated in minimum essential media containing 1% FBS for 14 h. Then, *Renilla* and firefly luciferase activities were measured in cell lysates using the Dual Luciferase Assay System (Promega, Madison, WI) with a Luminometer (Promega).

14. Measurement of ADP/ATP ratio

Cells were plated in clear-bottom white 96-well plates. After working time, the ADP/ATP ratio was determined using the EnzyLight ADP/ATP ratio assay kit (BioAssay Systems, Hayward, CA) according to the manufacturer's instructions. Briefly, addition of the ATP reagent to cells grown plate, and then luminescence of ATP (RLU A) was measured using a luminometer (Promega, Madison, WI). After 10 min, luminescence of background (RLU B) was measured. Next, addition of ADP reagent to the cells and luminescence due to ADP (RLU C) was measured. Finally, obtained the ADP/ATP was calculated by subtracting RLU B from RLU C and then dividing the result by RLU A.

15. Measurements of mitochondrial DNA

Total genomic DNA was extracted from HepG2 cells according to the protocol provided by

the manufacturer (Nucleogen, Siheung, Korea). Levels of cytochrome *c* oxidase subunit II (mtCOX II) transcribed from mitochondrial DNA (mtDNA) were quantified by real-time PCR. Nuclear-encoded receptor-interacting protein 140 (RIP140) was used as normailzation. The following primer pairs were used: human mtCOX II 5 -ACCTGCGACTCCTTGACGTTG-3 (forward) and 5 -TAGGACGATGGGCATGAAACTG-3 (reverse), and human RIP140 5 -GCTGGGCATAATGAAGAGGA-3 (forward) and 5 -CAAAGAGGCCAGTAATGTGCTATC-3 (reverse). Real-time PCR was performed using StepOne (Applied Biosystems, Foster City, CA) with a SYBR Green premix following the manufacturer's protocol (Applied Biosystems, Foster City, CA).

16. siRNA knockdown experiment

Cells were transfected with an siRNA directed against human SESN2 (Cat No. L-019134-02-0005, ON-TARGETplus SMARTpool; Dharmacon Inc., Lafayette, CO) or an siRNA directed against human AMPKα (Cat No. sc-45312, Santa Cruz Biotechnology, CA) using Lipofectamine 2000 (Invitrogen, San Diego, CA) for 24 h. A non-targeting control siRNA (100 pmol/mL) was used as negative control for all experiments. SESN2 and AMPKα knockdown was confirmed by immunoblot analysis.

17. Wound migration assay

Cells were seeded in 24-well plates and grown until 90% confluency in DMEM supplemented with 10% FBS. The monolayer was scratched straightly with a sterile 200 μL tip. The migration of cells to the cleared area was inspected under a microscope (magnification, 50×). Pictures were taken directly at the time of scratching and after scratching at 24 h. The

width of the injury line was measured by using Image J Software.

18. *In vitro* cell invasion/migration assay

An *in vitro* cell invasion assay was analysed in a BioCoat Matrigel Invasion Chamber (Becton-Dickinson, Bedford, MA) according to the protocol provided by the manufacturer. Briefly, the lower side of the Transwell was coated with Type I collagen (Corning, Bedford, MA). The lower compartment was filled with serum-free media containing 0.1% bovine serum albumin. Adenovirus infected HCT116 cells (2 X 10^4) were placed in the upper part of the Transwell, and incubated in DMEM with or without 10% FBS. 5-FU (50 μM) treatment was used as positive control. After 24 h, the non-invading cells on the upper side of the membrane were removed, and the invaded cells on the lower side of membrane were fixed with ice-cold methanol and then stained with 0.5% crystal violet (Sigma) for 20 min. Membrane was washed twice with distilled water, and allowed to air dry. The stained cells were visualized under a microscope (magnification, 100×). For quantification of cell invasion, membrane was dissolved in acetic acid. Then, absorbance at 570 nm was measured using a microplate reader (Spectramax 190, Molecular Device, Sunnyvale, CA). An *in vitro* cell migration assay was performed using an 8-μm polycarbonate filter Transwell (Costar, Lowel, MA) with 24-well plate. Experimental procedures the *in vitro* cell migration assay was the same as except that the filter was not coated with matrigel.

19. Statistical analysis

Multiple comparison tests for different groups were conducted and statistical significance was determined by one-way analysis of variance (ANOVA). The data were represented in the

form of means ± S.E., which was obtained from at least three independent experiments. The criterion for statistical significance was set at $p < 0.05$ or $p < 0.01$.

IV. RESULTS

Part I: Protection of mitochondrial function by Sestrin2 in glucose deprivation-induced cytotoxicity

1. Regulation of SESN2 expression by glucose level in hepatocytes

The first study determined whether glucose level regulates SESN2 expression in hepatocytes. Primary hepatocytes were isolated from mice after fasting or nonfasting for 18 h. The expression of SESN2 in primary hepatocytes from fasted mice was higher than primary hepatocytes from nonfasted mice (Fig. 1A, left). Deprivation of glucose resulted in upregluation of SESN2 protein level in hepatocyte-derived cell lines (AML12 and Huh7 cells) (Fig. 1A, right). In order to test whether glucose level affects on SESNs induction, HepG2 cells were incubated in various glucose concentrations (0–25 mM)-containing media, and then SESNs mRNA and protein level were measured. There were increases in the level of SESN2 mRNA and protein in glucose-free media (Fig. 1B and 1C). However, incubation of cells in high glucose (25 mM)-containing media did not change SESN2 expression when compared to normal glucose (5.6 mM) condition (Fig. 1B and 1C). Moreover, alteration of glucose concentration did not affect level of SESN1 mRNA (Fig. 1B). Upon glucose deprivation, the level of SESN2 mRNA significantly was increased starting at 6 h and peaked at 12 h, but SESN1 level was not changed (Fig. 1D). Also, glucose deprivation significantly increased the expression of SESN2 protein after 12 h and peaked at 18 h (Fig. 1E). To confirm the induction

of SESN2 by glucose deprivation, cells were transfected with a human SESN2-luciferase reporter plasmid and then incubated in glucose-free media. Exposure of cells to glucose-free medium resulted in a marked upregulation of reporter construct activity (Fig. 1F). Collectively, these results suggest that glucose deprivation upregulates transcriptional induction of SESN2.

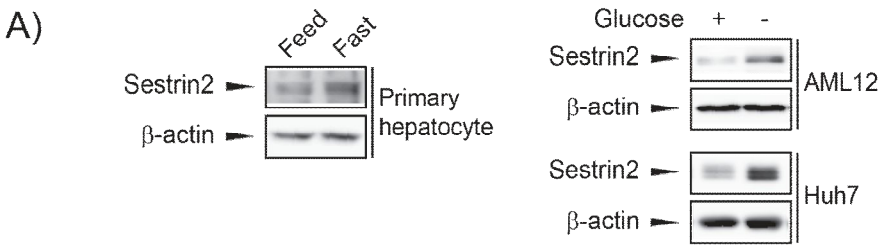

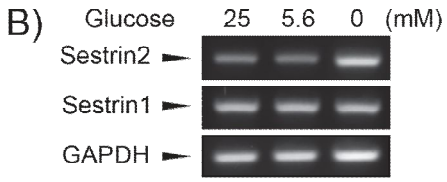

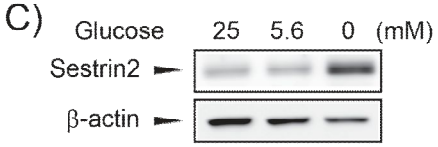

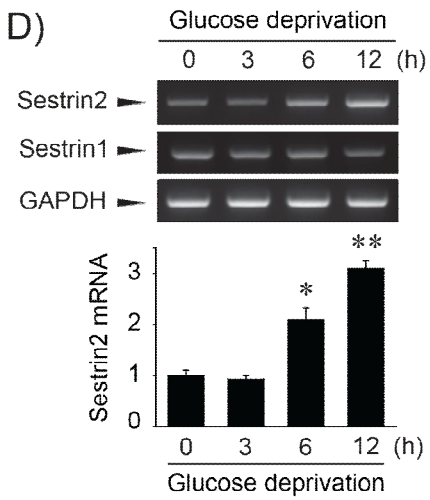

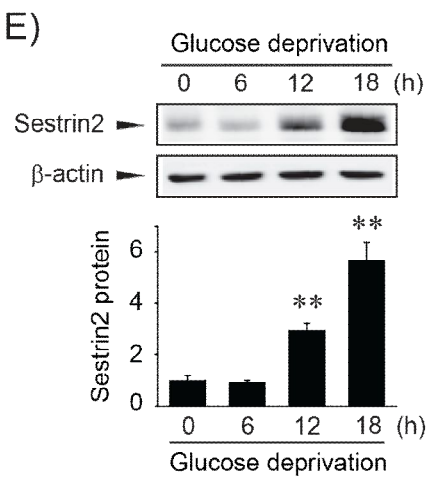

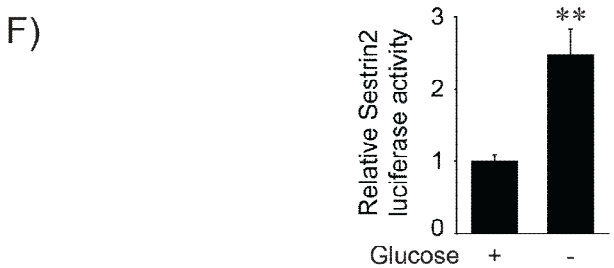

Fig. 1. Regulation of SESN2 expression by glucose level in hepatocytes

(A) Immunoblot analysis. SESN2 protein level was determined by using lysates from primary hepatocytes from mice that had fasted for 18 h (left). AML12 and Huh7 cells were incubated in glucose-containing (5.6 mM) or glucose-free DMEM for 18 h (right). Lysates from these cells were then used to determine SESN2 protein level via immunoblotting. The blots shown are representative of data from at least 3 different replicates.

(B) RT-PCR assays. HepG2 cells were incubated in the indicated concentrations of glucose for 6 h, and then the SESN1 or SESN2 transcripts were analyzed by RT-PCR. The results shown are representative of data from at least 3 different replicates.

(C) Immunoblot analysis. HepG2 cells were incubated in the indicated concentrations of glucose for 12 h. Lysates from these cells were then used to determine SESN2 protein level via immunoblotting. The blots shown are representative of data from at least 3 different replicates.

(D) RT-PCR assays. HepG2 cells were incubated in glucose-free DMEM for the indicated time period (0–12 h). SESN1 or SESN2 transcripts were then analyzed by RT-PCR. The results shown are representative of data from at least 3 different replicates; $^{*}p < 0.05$ or $^{**}p < 0.01$ when compared to the control.

(E) Immunoblot analysis. The lysates of cells incubated in glucose-free DMEM for 0–18 h were immunoblotted for SESN2 protein level. The blots shown are representative of data from at least 3 different replicates; $^{**}p < 0.01$ when compared to the control.

(F) Luciferase activity. SESN2 luciferase activity was determined from the cell lysates incubated in glucose-free DMEM for 12 h. Data were expressed as the mean ± S.E. from at least 3 different replicates; $^{**}p < 0.01$ when compared to the glucose-incubated control.

2. The effects of glucose deprivation-induced ROS in SESN2 expression

Previous study showed that SESN2 is induced by oxidative stress and an siRNA knockdown of SESN2 increases cell death mediated by hydrogen peroxide (Shin et al, 2012). In addition, recent studies showed that SESN2 protects diverse cells against oxidative stress (Chen et al, 2014; Seo et al, 2014; Yang et al, 2014). Thus, this study determined whether excess production of ROS by glucose deprivation is involved in SESN2 induction. First, to examine the effect of glucose deprivation on ROS production, intracellular ROS accumulation was analyzed using DCFH-DA. An increase of intracellular ROS was observed under glucose deprivation (Fig. 2A). To confirm that overproduction of ROS are the cause of glucose deprivation-induced SESN2 upregulation, cells were treated with various ROS scavengers with glucose-free medium. Treatment with NAC (an antioxidant), Mn-TBAP (a novel SOD mimetic agent), or rotenone (a mitochondrial complex I inhibitor) significantly inhibited the induction of SESN2 expression by glucose deprivation (Fig. 2B and 2C). These results support our conclusion that glucose deprivation increases ROS production, which in turn induces SESN2 expression.

It is well established that increased ROS induce various antioxidant genes via activation of ARE. Shin et al. demonstrated that ROS cause SESN2 induction, which is affected by Nrf2-ARE activation (Shin et al, 2012). In addition, Lee et al. reported that glucose deprivation causes Nrf2 activation and induces heme oxygenase-1 (HO-1) expression in HepG2 cells (Lee et al, 2010a). The hypothesis that activation of Nrf2 could lead to induction of SESN2 expression under glucose deprivation was examined. Incubation of glucose-free medium increased the phosphorylation of Nrf2 (Fig. 3A), which represents increase of Nrf2 stabilization and enables Nrf2 to translocate to nucleus (Niture et al, 2014). To elucidate the role of ARE in

SESN2 induction from glucose deprivation, cells were transfected with the ΔARE in the SESN2 reporter construct. A specific deletion of the ARE in the SESN2 promoter region markedly reduced the activity of the SESN2 reporter construct in glucose deprivation (Fig. 3B). These observations indicate that Nrf2-ARE system was involved in SESN2 induction under glucose deprivation. Overall, upregulation of SESN2 induction is involved in activation of Nrf2-ARE by glucose deprivation.

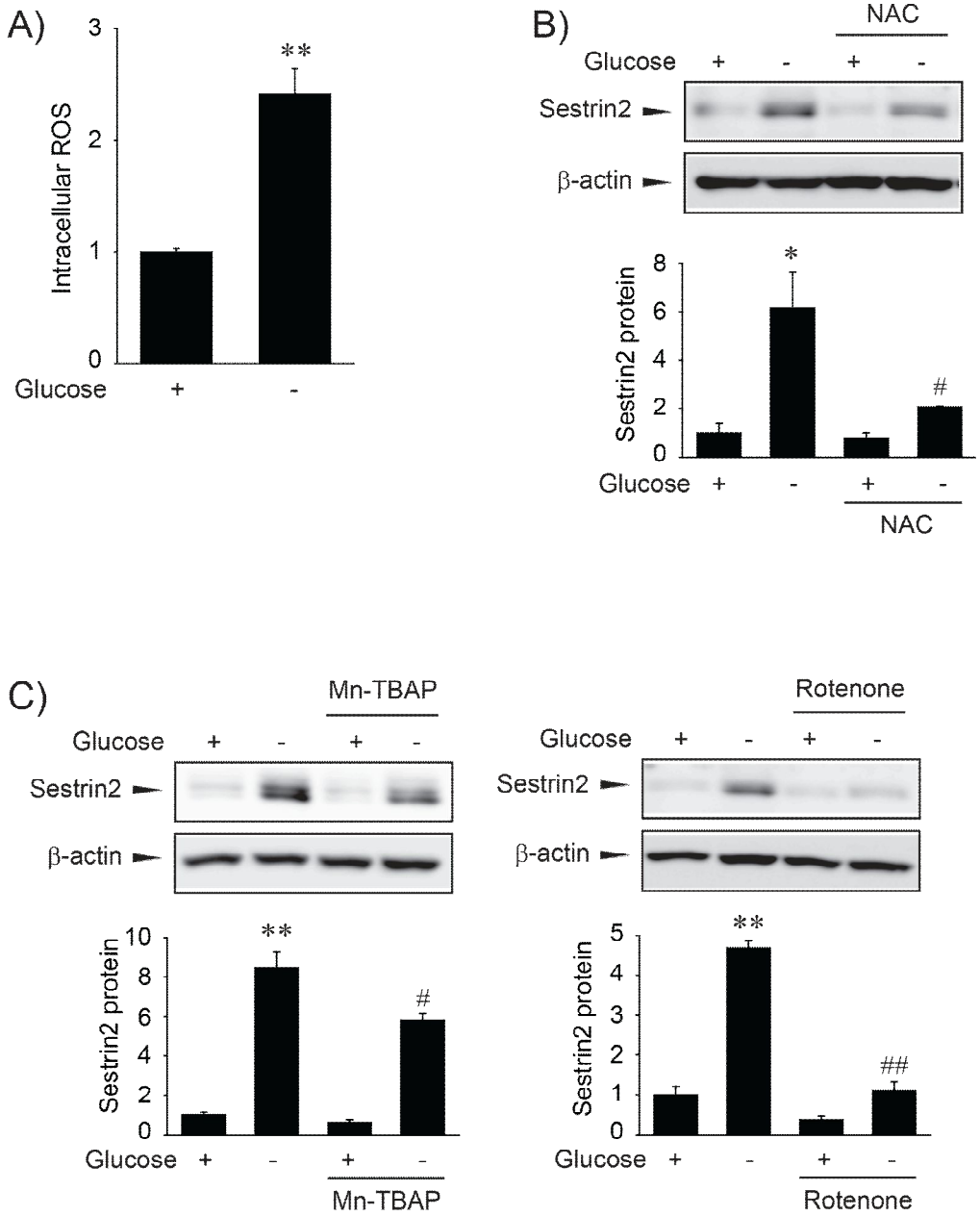

Fig. 2. The effects of glucose deprivation-induced ROS in SESN2 expression

(A) Measurement of ROS production. Cells were incubated in glucose (5.6 mM) or glucose-free DMEM for 12 h. ROS production was assessed by DCF fluorescent intensity. The data are expressed as mean ± S.E. from at least 3 different replicates; $^{**}p < 0.01$ when compared to the glucose-incubated control.

(B) Immunoblot analysis. Cells were incubated with or without NAC (5 mM) in glucose (5.6 mM) or glucose-free DMEM for 12 h. Then, lysates from these cells were used to determine SESN2 protein level via immunoblotting. The blots shown are representative of data from at least 3 different replicates; $^{*}p < 0.05$ when compared to the glucose-incubated control; $^{\#}p < 0.05$ when compared to cells incubated in glucose-free DMEM without NAC.

(C) Immunoblot analysis. Cells were incubated with or without Mn-TBAP (20 μM, left) or rotenone (10 nM, right) in glucose (5.6 mM) or glucose-free DMEM for 12 h. Then, lysates from these cells were used to determine SESN2 protein level via immunoblotting. The blots shown are representative of data from at least 3 different replicates; $^{**}p < 0.01$ when compared to the glucose-incubated control; $^{\#}p < 0.05$ or $^{\#\#}p < 0.01$ when compared to cells incubated in glucose-free DMEM without Mn-TBAP or rotenone.

A)

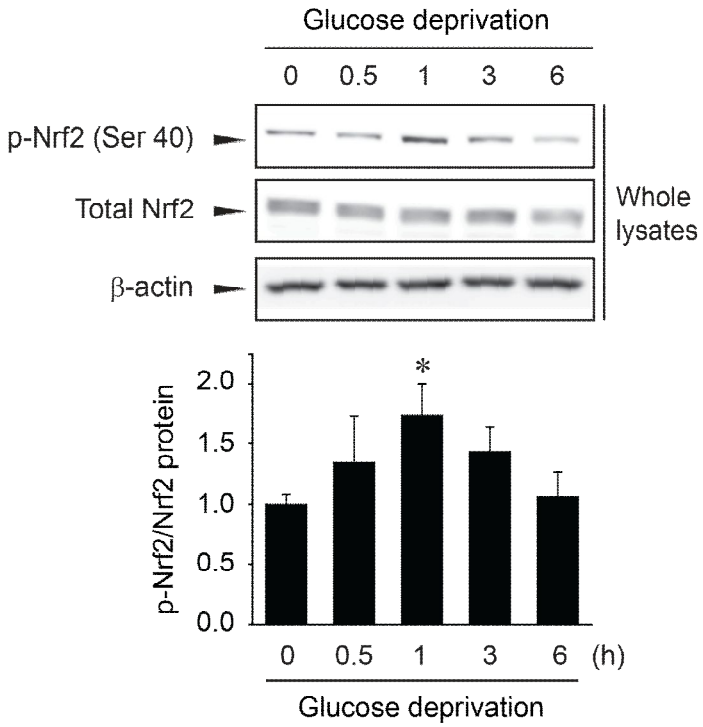

B)

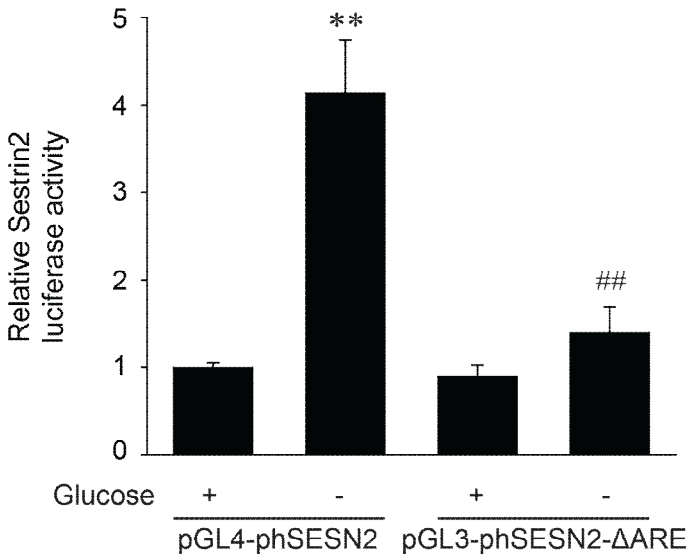

Fig. 3. Involvement of Nrf2 activation in glucose deprivation-induced SESN2 induction

(A) Immunoblot analysis. The lysates of cells incubated in glucose-free DMEM for 0–6 h were immunoblotted. The blots shown are representative of data from at least 3 different replicates; $^{*}p < 0.05$ when compared to the control.

(B) Luciferase activity. Cells had been transfected with pGL4-phSESN2 or pGL3-phSESN2-ΔARE and incubated in glucose (5.6 mM) or glucose-free DMEM for 12 h. Luciferase activity was determined from the cell lysates. Data were expressed as the mean ± S.E. from at least 3 different replicates; $^{**}p < 0.01$ when compared to the glucose-incubated control in pGL4-phSESN2 transfected cells; $^{\#\#}p < 0.01$ when compared to cells incubated in glucose-free DMEM after pGL4-phSESN2 transfection.

3. Glucose deprivation-induced mitochondrial damage and apoptosis

In HepG2 cells, depletion of glucose markedly increases apoptosis (Lee et al, 2010a). Since glucose deprivation increased mitochondrial ROS and depleted ATP, cells cannot maintain mitochondrial membrane permeability and lead to activate the apoptotic signal cascade (De Saedeleer et al, 2014; Moley and Mueckler, 2000). Therefore, in an attempt to investigate the linkage between glucose deprivation-induced cytotoxicity and mitochondrial damage, mitochondrial membrane permeability was assessed by using rhodamine 123 staining. Glucose deprivation reduced intensity of rhodamine 123 fluorescence in cells, but cyclosporin A, inhibitor of mitochondrial membrane transition pore formation (Petronilli et al, 2001; Scorrano et al, 2001; Shin and Kim, 2009), restored decreased in intensity of rhodamine 123 fluorescence (Fig. 4A); this result represents that glucose deprivation increased the mitochondrial membrane damage. The recovery of mitochondria membrane potential by cyclosporin A also antagonized glucose deprivation-induced cell death (Fig. 4B). Moreover, trolox (a water soluble analogue of vitamin E and hydroxyl radical scavenger), catalase (a hydrogen peroxide scavenger), and Mn-TBAP significantly protected cells death against glucose deprivation (Fig. 4C). This result indicates that intracellular ROS including mitochondria-derived ROS might be involved glucose deprivation-induced cytotoxicity. Collectively, these results suggested that glucose deprivation induces the overproduction of ROS, which leads to cell death.

A)

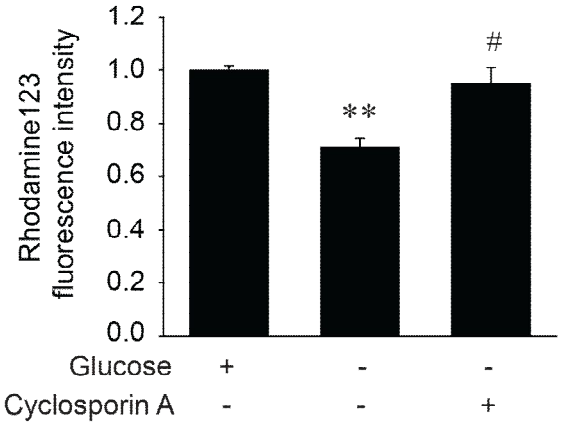

B)

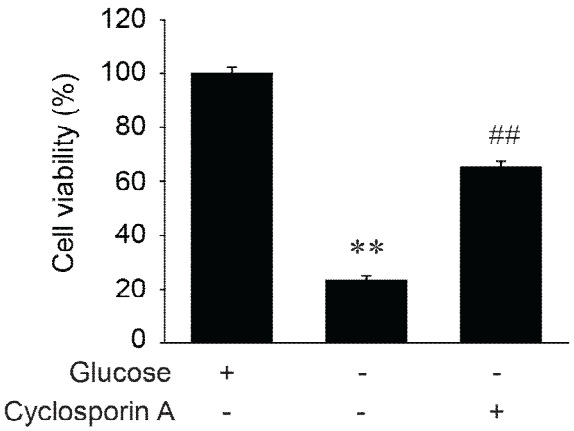

C)

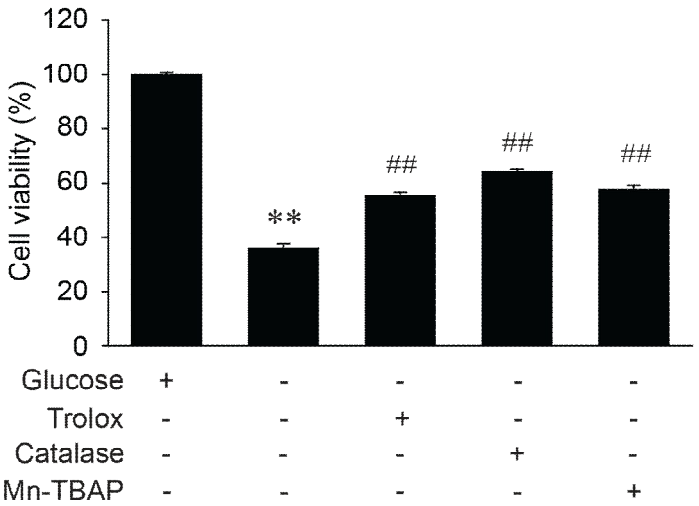

Fig. 4. Glucose deprivation-induced mitochondrial damage and apoptosis

(A) Measurement of mitochondrial membrane permeability changes. Cells were incubated in the indicated DMEM with or without cyclosporin A (10 μg/mL) for 18 h. Data represent the mean ± S.E. of data from at least 3 different replicates; $^{**}p < 0.01$ when compared to the glucose-incubated control; $^{\#}p < 0.05$ when compared to cells incubated in glucose-free DMEM without cyclosporin A.

(B) Cell viability assay. Cells were incubated in indicated DMEM without or with cyclosporin A (10 μg/mL) for 24 h. The effect of cyclosporin A on cell viability was then assessed using MTT assay. Data are expressed as the means ± S.E. of data from at least 3 different replicates; $^{**}p < 0.01$ when compared to the glucose-incubated control; $^{\#\#}p < 0.01$ when compared to cells incubated in glucose-free DMEM without cyclosporin A.

(C) Cell viability assay. Cells were incubated in indicated DMEM with or without trolox (100 μM), PEG-catalase (catalase, 1000 U/mL), or Mn-TBAP (20 μM) for 24 h. The effect of these antioxidants on cell viability was then assessed using the MTT assay. The data are expressed as the means ± S.E. of data from at least 3 different replicates; $^{**}p < 0.01$ when compared to the glucose-incubated control; $^{\#\#}p < 0.01$ when comparing treatment groups under glucose-free DMEM incubation.

4. The effects of SESN2 overexpression on glucose deprivation-induced cytotoxicity

To verify whether SESN2 has cytoprotective activity, HepG2 cells that stably overexpressed SESN2 were prepared. Overexpression of SESN2 was verified by immunoblot analysis (Fig. 5A, upper). Overexpression of SESN2 repressed glucose deprivation-induced cell death compared to MOCK-transfected cells (Fig. 5A, lower). To examine whether glucose deprivation-induced cytotoxicity was related with the induction of apoptosis, cell lysates were immunoblotted for marker proteins for apoptotic death. Glucose deprivation induced PARP cleavage, caspase-3 activation and decrease in Bcl-x_L expression. However, SESN2 overexpression prevented PARP and caspase-3 cleavage and a decrease Bcl-x_L expression from glucose deprivation (Fig. 5B). Indeed, SESN2-overexpressed cells attenuated glucose deprivation-induced ROS production (Fig. 5C). These results clearly indicate that SESN2 inhibits glucose deprivation-induced ROS production, thereby preventing apoptosis.

A)

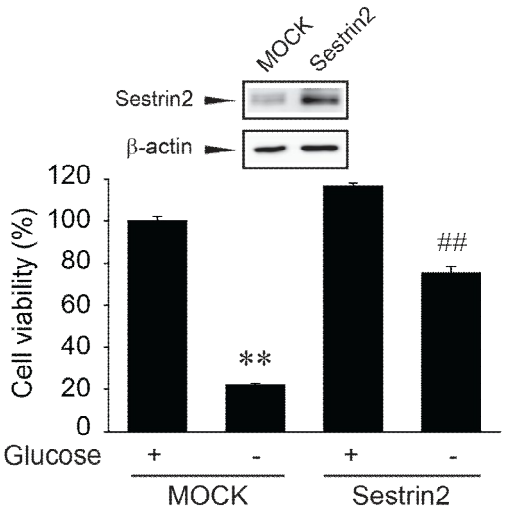

B)

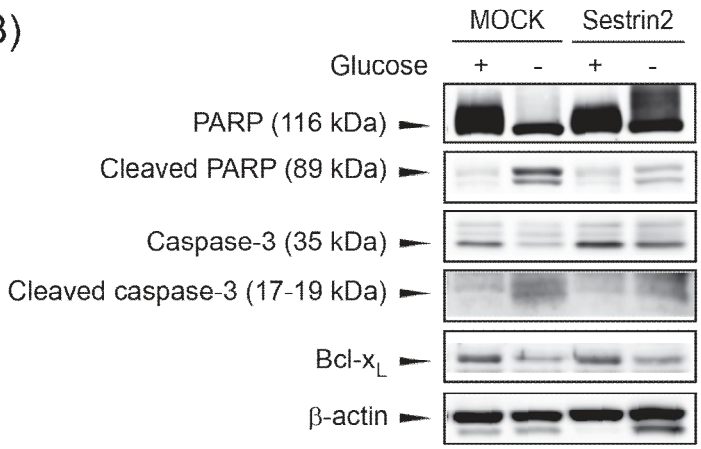

C)

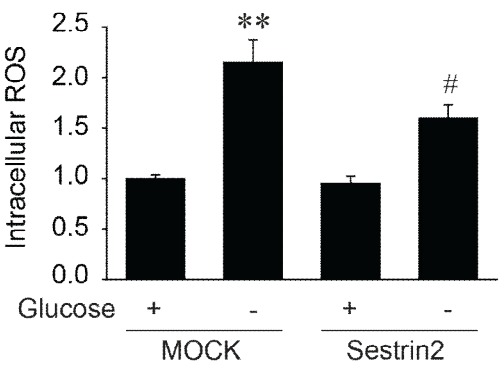

Fig. 5. The effects of SESN2 overexpression on glucose deprivation-induced cytotoxicity

(A) Cell viability assay. Cells were incubated in DMEM with glucose (5.6 mM) or glucose-free DMEM for 24 h. Cell death was determined by the MTT assay. Data represent the mean ± S.E. of at least 3 different replicates; $^{**}p < 0.01$ when compared to glucose-incubated MOCK-transfected cells; $^{\#\#}p < 0.01$ when comparing MOCK-transfected cells and SESN2-overexpressing cells in glucose free-DMEM.

(B) Immunoblot analysis. Cells were incubated in DMEM with glucose (5.6 mM) or glucose-free DMEM for 24 h. Then, lysates from these cells were used to determine levels of apoptotic proteins via immunoblotting. The blots shown are representative of data from at least 3 different replicates.

(C) Measurement of ROS generation. Cells were incubated in DMEM with glucose (5.6 mM) or glucose-free DMEM for 12 h. ROS levels were then assessed via DCF fluorescent intensity. Data represent the mean ± S.E. of data from at least 3 different replicates; $^{**}p < 0.01$ when compared to glucose-incubated MOCK-transfected cells; $^{\#}p < 0.05$ when comparing MOCK-transfected cells and SESN2-overexpressing cells in glucose free-DMEM.

5. The effects of SESN2 overexpression on glucose deprivation-induced mitochondrial damage

Next, the possibility that SESN2 could protect mitochondrial dysfunction against glucose deprivation was determined. Increased ADP/ATP ratio revealed that glucose-free media incubation in MOCK-transfected cells significantly induced mitochondrial dysfunction (Fig. 6A). In contrast, overexpression of SESN2 significantly decreased ADP/ATP ratio when compared with MOCK-transfected cells (Fig. 6A). In addition, glucose deprivation significantly decreased mtDNA, a copy number of mitochondrial DNA, in MOCK-transfected cells, but SESN2 overexpressed cells effectively restored mtDNA by glucose deprivation (Fig. 6B). Moreover, glucose deprivation decreased mitochondria membrane potential in MOCK-transfected cells, but this decrease was prevented by SESN2 overexpression; this result suggests that SESN2 inhibits mitochondrial membrane damage (Fig. 6C). Likewise, to assess the functional role of SESN2 in the maintenance of mitochondrial membrane potential, transfection with an siRNA directed against human SESN2 was conducted. Knockdown of SESN2 was confirmed by immunoblot analysis (Fig. 6D, upper). The protective effect of SESN2 in mitochondrial membrane permeability transition by glucose deprivation was reversed by siRNA knockdown of SESN2 (Fig. 6D, lower). These results clearly indicate that SESN2 contributes to restoration of mitochondrial function after glucose deprivation-induced oxidative stress.

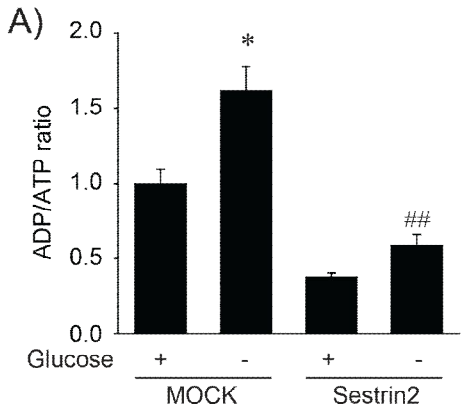

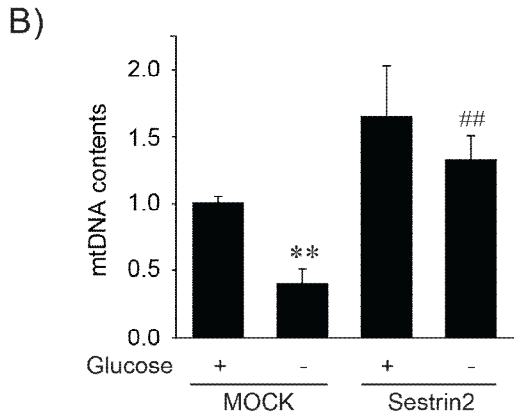

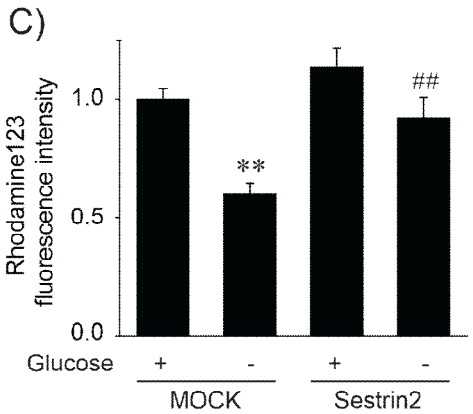

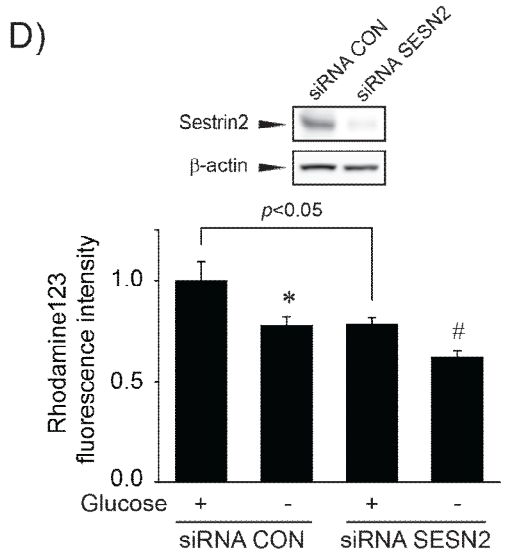

Fig. 6. The effects of SESN2 overexpression on glucose deprivation-induced mitochondrial damage

(A) ADP/ATP ratio assay. Cells were incubated in DMEM with glucose (5.6 mM) or glucose-free DMEM for 15 h. Data represent the mean ± S.E. of data from at least 3 different replicates; $^{*}p < 0.05$ when compared to glucose-incubated MOCK-transfected cells; $^{\#\#}p < 0.01$ when comparing MOCK-transfected cells and SESN2-overexpressing cells in glucose free-DMEM.

(B) mtDNA contents. Cells were incubated in DMEM with glucose (5.6 mM) or glucose-free DMEM for 15 h. The samples were then subjected to real-time PCR analysis with primers for the mtDNA region COXII. Data represent the mean ± S.E. of data from at least 3 different replicates; $^{**}p < 0.01$ when compared to glucose-incubated MOCK-transfected cells; $^{\#\#}p < 0.01$ when comparing MOCK-transfected cells and SESN2-overexpressing cells in glucose free-DMEM.

(C) Measurement of mitochondrial membrane permeability changes. Cells were incubated in DMEM containing glucose (5.6 mM) or glucose-free DMEM for 18 h. Data represent the mean ± S.E. of data from at least 3 different replicates; $^{**}p < 0.01$ when compared to glucose-incubated MOCK-transfected cells; $^{\#\#}p < 0.01$ when comparing MOCK-transfected cells and SESN2-overexpressing cells in glucose free-DMEM.

(D) Measurement of mitochondrial membrane permeability changes. Cells were transfected with control siRNA (siRNA CON) or SESN2 siRNA (siRNA SESN2). Then, cells were incubated in DMEM containing glucose (5.6 mM) or glucose-free DMEM for 12 h; $^{*}p < 0.05$ when compared to glucose-incubated control siRNA-transfected cells; $^{\#}p < 0.05$ when comparing control siRNA-transfected cells and SESN2 siRNA-transfected cells in glucose free-DMEM.

6. Inhibition of glucose deprivation-induced mitochondrial dysfunction by SESN2–AMPK activation

Previous studies have shown that the cytoprotective effects of SESN2 result from activation of AMPK during various stress (Ben-Sahra et al, 2013; Budanov and Karin, 2008; Sanli et al, 2012). In addition, AMPK could protect cells against mitochondrial dysfunction (Ido et al, 2002). Therefore, the role of SESN2–AMPK axis in protecting mitochondrial dysfunction under glucose deprivation was investigated. First, the effects of glucose deprivation on the timed responses of ACC and AMPK phosphorylation in cells were examined. Glucose deprivation increased the phosphorylation of ACC, which represents cellular AMPK activity (Fig. 7A). Overexpression of SESN2 similarly the increase of ACC phosphorylation compared with MOCK-transfected cells by glucose deprivation (Fig. 7B). Next, to examine the role of AMPK activation by SESN2 in protecting mitochondrial function, cells were transfected with a DN-AMPK. Overexpression of the DN-AMPK was confirmed by level of AICAR-induced ACC phosphorylation (Fig. 7C, upper). The recovery of decrease in mitochondrial membrane permeability elicited by SESN2 overexpression was notably reversed by DN-AMPK overexpression (Fig. 7C, lower). In another effort to verify the role of AMPK in the protection of cell death, the effect of AICAR (an AMPK activator) on cell viability was determined (Fig. 7D). AICAR treatment attenuated the glucose deprivation-induced increases in cell death. These results provide evidence that the cytoprotective effect and the recovery of mitochondrial function by SESN2 might be associated in part with AMPK activation.

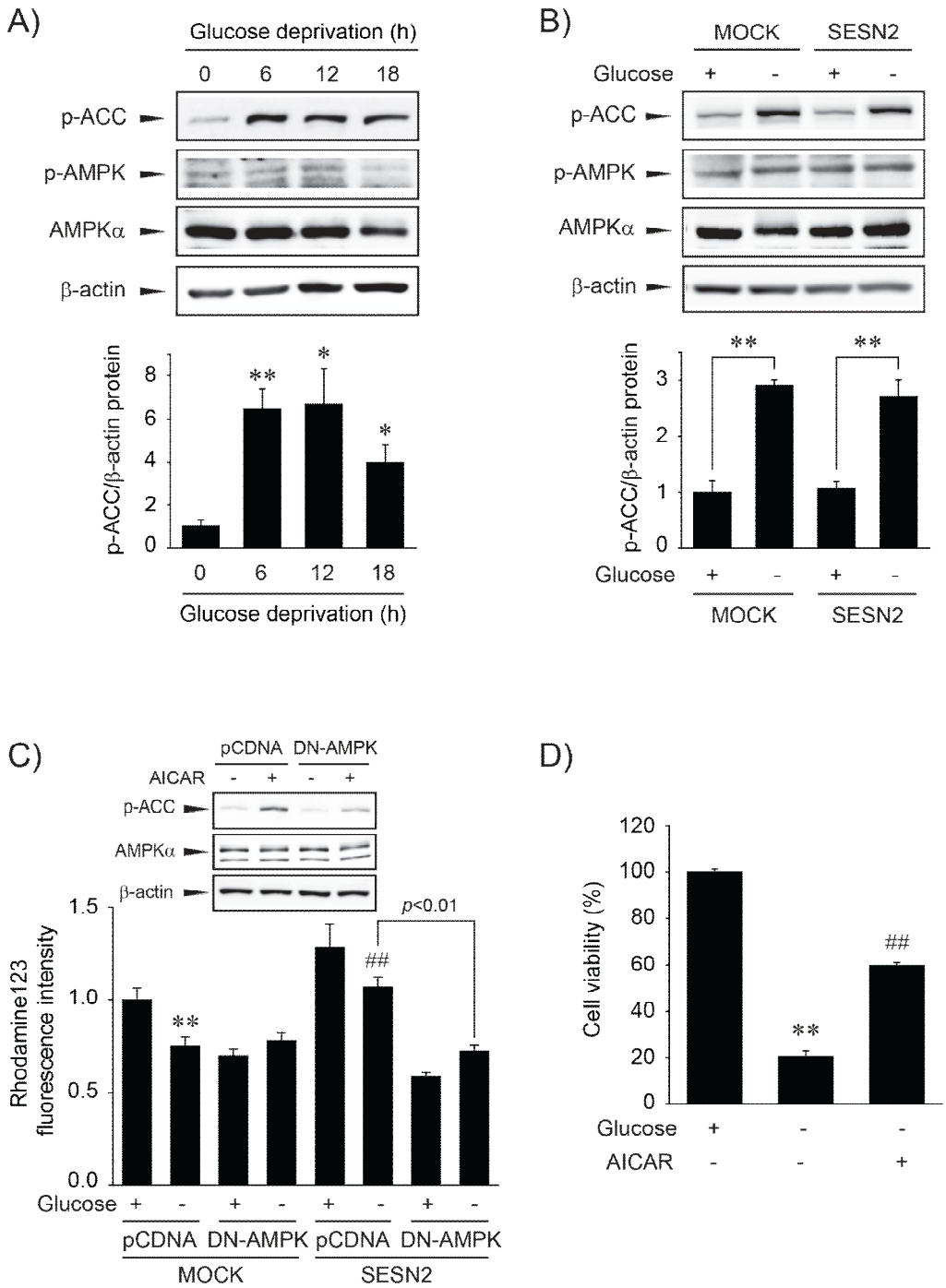

Fig. 7. Inhibition of glucose deprivation-induced mitochondrial dysfunction by SESN2–AMPK activation

(A) Immunoblot analysis. The lysates of cells that had been incubated in glucose-free DMEM for 0–18 h were immunoblotted. The blots shown are representative of data from at least 3 different replicates; $^{*}p < 0.05$ or $^{**}p < 0.01$ when compared to the control.

(B) Immunoblot analysis. Cells were incubated in DMEM containing glucose (5.6 mM) or glucose-free DMEM for 12 h. Protein levels in lysates from these cells were then determined via immunoblotting. Data represent the mean ± S.E. of data from at least 3 different replicates; $^{**}p < 0.01$ when compared to glucose-incubated each control cells.

(C) Measurement of mitochondrial membrane permeability changes. MOCK-transfected or SESN2-overexpressing cells were transfected with a construct expressing a dominant-negative form of AMPK (DN-AMPK) or pCDNA (i.e., empty plasmid). Then, cells were incubated in DMEM containing glucose (5.6 mM) or glucose-free DMEM for 12 h. Data represent the mean ± S.E. of data from at least 3 different replicates; $^{**}p < 0.01$ when compared to glucose-incubated pCDNA and mock-transfected cells; $^{\#\#}p < 0.01$ when comparing pCDNA and MOCK-transfected cells and pCDNA transfected SESN2 overexpressing cells in glucose free-DMEM.

(D) Cell viability assay. Cells were incubated with or without AICAR (2 mM) in indicated DMEM for 24 h. The effect of AICAR on cell viability was then assessed using the MTT assay. The data were expressed as means ± S.E. of data from at least 3 different replicates; $^{**}p < 0.01$ when compared to the glucose-incubated control; $^{\#\#}p < 0.01$ when compared to cells incubated in glucose-free DMEM without AICAR.

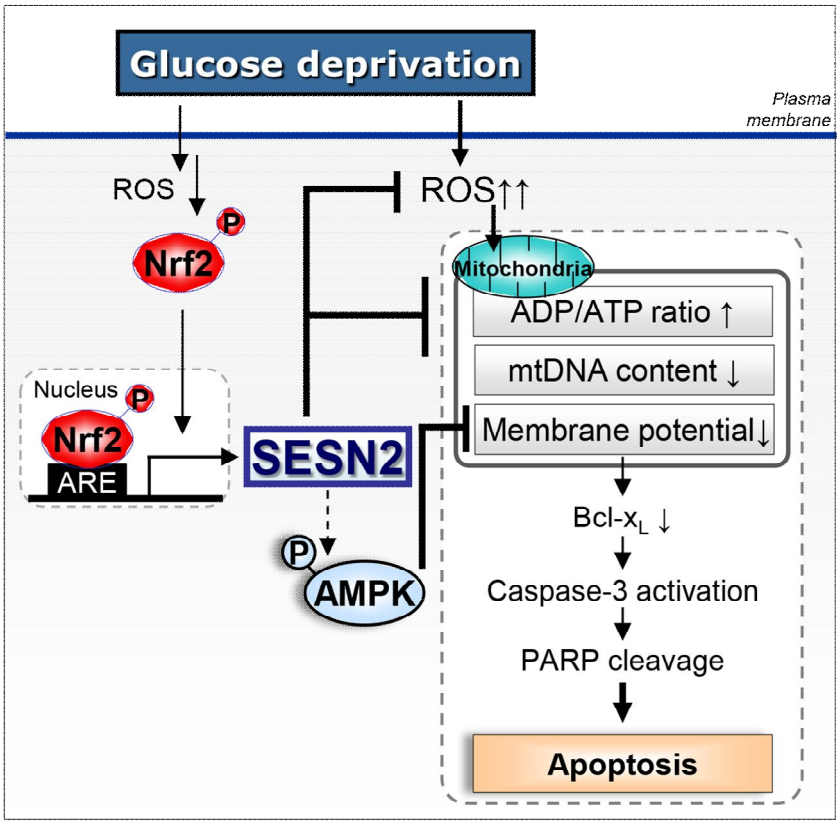

Fig. 8. Schematic diagram illustrating that SESN2 inhibits mitochondrial dysfunction and apoptosis against glucose deprivation-induced stress by AMPK activation.

Part II: Sestrin2 inhibits HIF-1α accumulation through increase of PHD activity and H_2O_2-scavenging effect

1. Inhibition of HIF-1α accumulation by SESN2 overexpression

Hypoxia induces HIF-1α accumulation, which contributes cancer cells to adapt to microenvironments (Denko, 2008; Keith et al, 2012). The second study investigated whether SESN2 inhibits the HIF-1α-mediated adaptive response in cancer cells. First, to demonstrate the role of SESN2 in HIF-1α level, HEK293 cells were transfected with HIF-1α and/or SESN2 expression plasmid. When cells were transfected with HIF-1α, an increase in HIF-1α level was observed (Fig. 9A). However, SESN2 overexpression significantly repressed HIF-1α level in HEK293 cells (Fig. 9A). Next, to elucidate whether SESN2 inhibits HIF-1α accumulation in colorectal cancer cells, HCT116 and HT29 cells were exposed to hypoxia (1% O_2) or normoxia (21% O_2). Hypoxia significantly accumulated HIF-1α protein for 3 h in both Ad-LacZ (control)-infected HCT116 (Fig. 9B, left) and HT29 (Fig. 9B, right) cells. However, Ad-SESN2 infection notably diminished hypoxia-induced HIF-1α accumulation in HCT116 (Fig. 9B, left) and HT29 (Fig. 9B, right) cells. The inhibitory effect of SESN2 on HIF-1α accumulation was confirmed by $CoCl_2$ (a hypoxia mimetic agent) treatment. Treatment of cells with $CoCl_2$ resulted in a marked increase in HIF-1α accumulation for 3–6 h in Ad-GFP (control)-infected HCT116 cells (Fig. 9C, left) and for 3 h in HT29 cells (Fig. 9C, right). The accumulation of HIF-1α by $CoCl_2$ treatment was significantly suppressed by Ad-SESN2 infection in HCT116 (Fig. 9C, left) and HT29 (Fig. 9C, right) cells; overexpression of the

SESN2 was verified by observation of SESN2 expression (Fig. 9C). These results indicate that SESN2 inhibits HIF-1α accumulation under hypoxia.

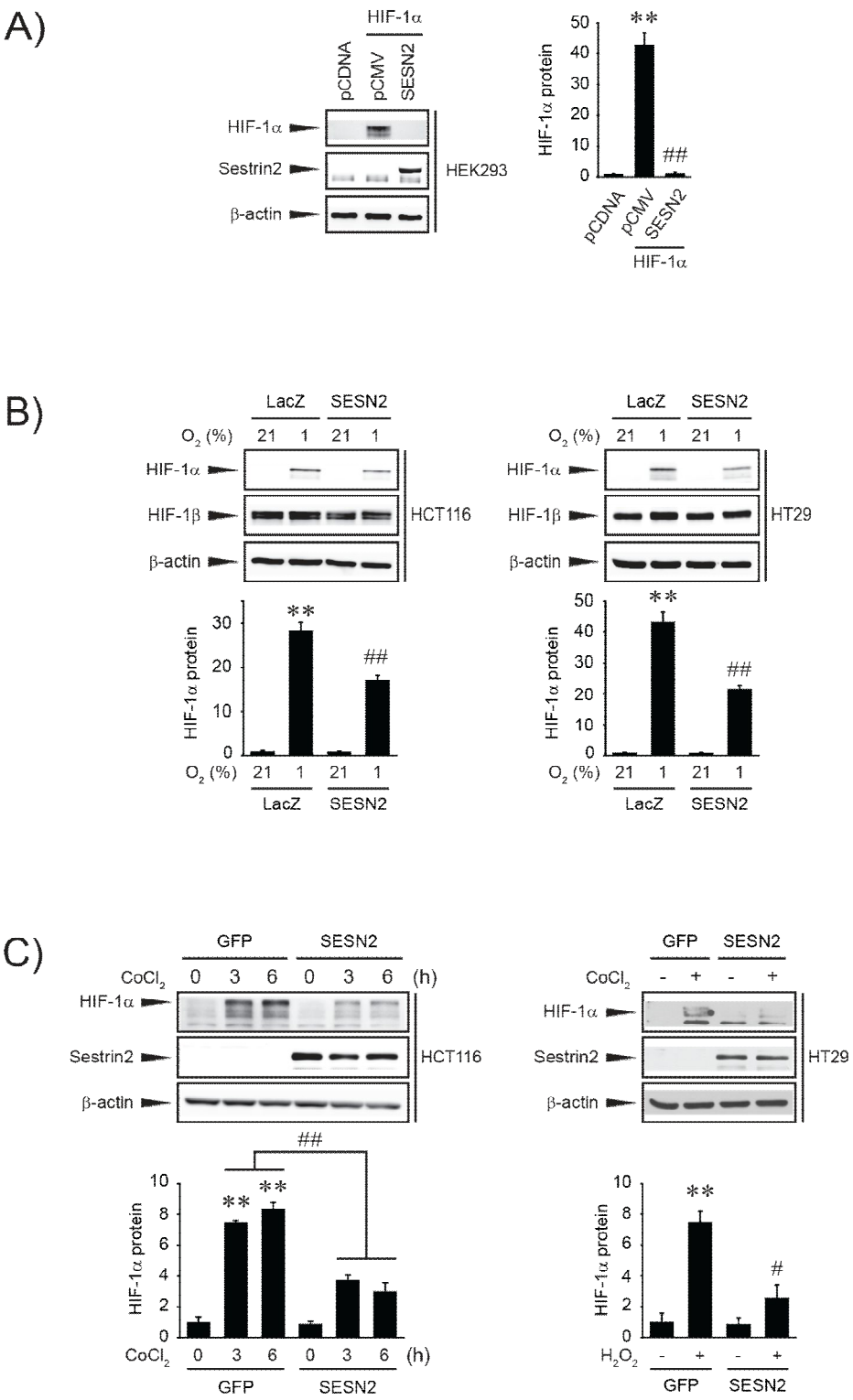

Fig. 9. Inhibition of HIF-1α accumulation by SESN2 overexpression

(A) Immunoblot analysis. HEK293 cells were transfected with pCDNA-HIF-1α or either pCMV-tag3A (pCMV) or SESN2, together with pCDNA-HIF-1α for 48 h. Lysates from these cells were then used to determine protein level via immunoblotting. The blots shown are expressed as the mean ± S.E. from at least 3 independent experiments; $^{**}p < 0.01$ when compared to the pCDNA-transfected cells; $^{\#\#}p < 0.01$ when compared to the pCMV and SESN2-transfected cells.

(B) Immunoblot analysis. HCT116 (left) or HT29 (right) cells were incubated under the condition of normoxia (21% oxygen) or hypoxia (1% oxygen) for 3 h after Ad-LacZ or Ad-SESN2 infection. Lysates from these cells were then used to determine protein level via immunoblotting. The blots shown are expressed as the mean ± S.E. from at least 3 independent experiments; $^{**}p < 0.01$ when compared to the normoxia-incubated control in Ad-LacZ-infected cells; $^{\#\#}p < 0.01$ when compared to the hypoxia-incubated Ad-LacZ-infected cells.

(C) Immunoblot analysis. HCT116 (left) or HT29 (right) cells exposed to $CoCl_2$ (100 μM) for 0–6 h (left) or 3 h (right) after Ad-GFP or Ad-SESN2 infection. Lysates from these cells were then used to determine protein level via immunoblotting. The blots shown are expressed as the mean ± S.E. from at least 3 independent experiments; $^{**}p < 0.01$ when compared to the vehicle-treated control in Ad-GFP-infected cells; $^{\#}p < 0.05$ or $^{\#\#}p < 0.01$ when compared to the $CoCl_2$-treated Ad-GFP-infected cells.

2. Inhibition of HIF-1α-dependent gene transcription by SESN2 overexpression

HIF-1α makes a complex with HIF-1β to form a heterodimer (Wang et al, 1995; Wenger et al, 1997). HIF-1α/β complex is translocated into the nucleus and induces target genes involved in angiogenesis and glycolysis in cancer cells (Giaccia et al, 2003; Lee et al, 2009b). To observe effects of SESN2 on HIF-1α-dependent gene transcription, a luciferase reporter assay in the human lungcarcinoma cell line, A549 cells which had been stably transfected with a HRE reporter construct was performed. HRE-luciferase activity was increased by $CoCl_2$ treatment for 24 h in Ad-GFP-infected A549 cells, but Ad-SESN2 infection decreased HRE reporter activity (Fig. 10A, left); overexpression of the SESN2 was verified by immunoblot analysis (Fig. 10A, right). Consistently, $CoCl_2$ treatment increased the level of GLUT1, VEGF, CA-IX, LDH A and PDK1 in HCT116 (Fig. 10B, upper) and HT29 (Fig. 10B, lower) cells. The increased HIF-1α-target genes have been studied as cellular markers for hypoxia. However, Ad-SESN2 significantly decreased the $CoCl_2$-induced transcripts of GLUT1, VEGF, CA-IX, LDH A and PDK1 in HCT116 (Fig. 10B, upper) and HT29 (Fig. 10B, lower) cells. These results show that SESN2 inhibits HIF-1α-mediated gene regulation in colon cancer cells.

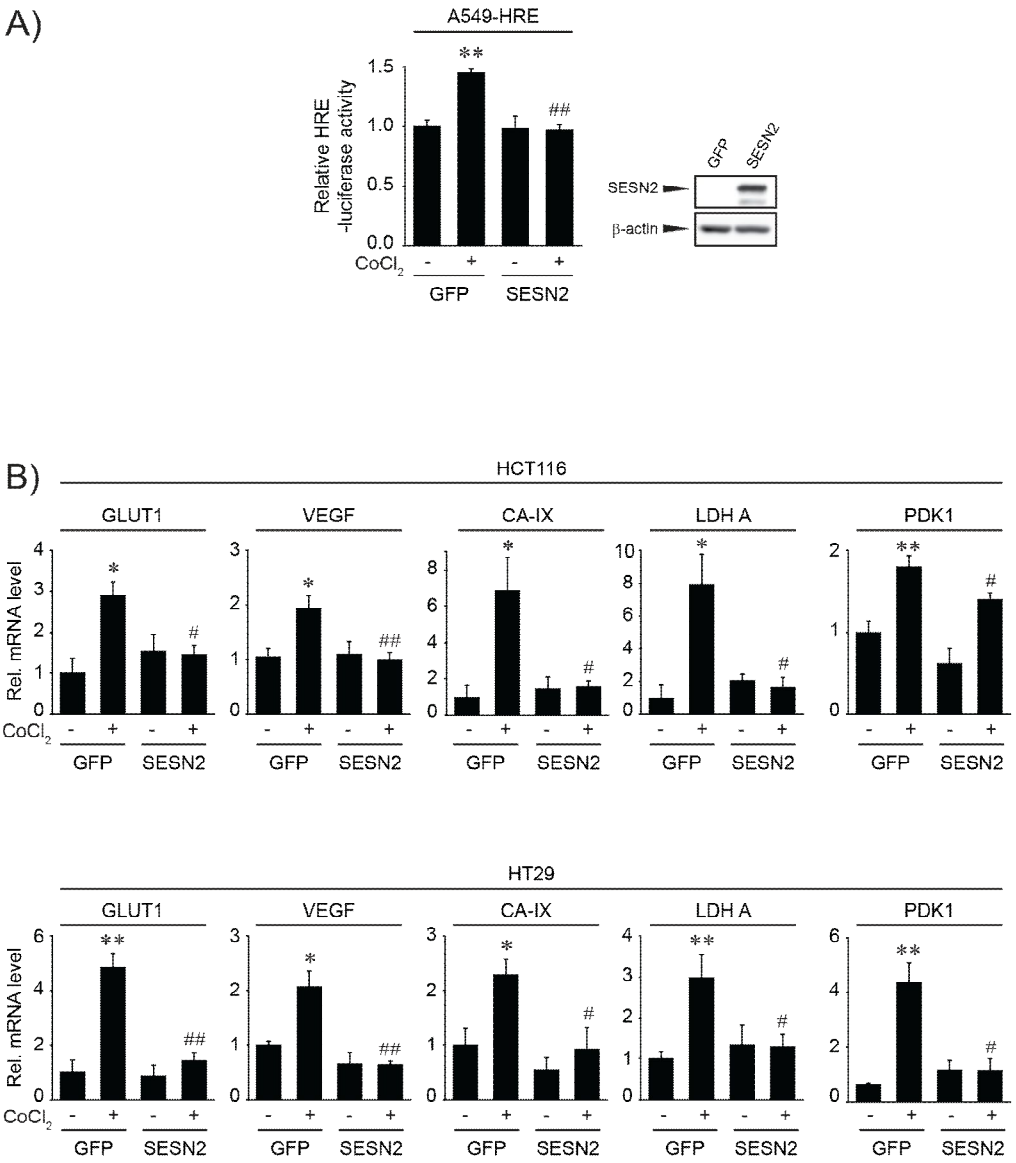

Fig. 10. Inhibition of HIF-1α-dependent gene transcription by SESN2 overexpression

(A) HRE reporter gene assay. HRE-A549 cells were incubated with $CoCl_2$ (100 μM) for 24 h following Ad-GFP or Ad-SESN2 infection. Luciferase activity was measured in the cell lysates. Data were expressed as the mean ± S.E. from at least 3 different replicates; $^{**}p < 0.01$ when compared to the vehicle-treated control in Ad-GFP-infected cells; $^{\#\#}p < 0.01$ when compared to the $CoCl_2$-treated Ad-GFP-infected cells.

(B) Real-time PCR assays. HCT116 (upper) or HT29 (lower) cells exposed to $CoCl_2$ (100 μM) for 6 h (upper) or 3 h (lower) after Ad-GFP or Ad-SESN2 infection. Data were expressed as the mean ± S.E. from at least 3 different replicates; $^{*}p < 0.05$ or $^{**}p < 0.01$ when compared to the vehicle-treated control in Ad-GFP-infected cells; $^{\#}p < 0.05$ or $^{\#\#}p < 0.01$ when compared to the $CoCl_2$-treated Ad-GFP-infected cells.

3. Inhibition of *in vitro* cell migration and invasion by SESN2 overexpression

HIF-1α activation induces cell growth, migration, and invasion in cancer cells (Denko, 2008; Keith et al, 2012; Semenza, 2008; 2014). The ability of cancer cells to disseminate from the primary site and form distant metastases is the main cause for cancer-related morbidity in patients with solid tumors (Denko, 2008; Popovic et al, 2014). Therefore, much effort has been invested in the identification of the HIF-1α signaling pathways and the cellular structures involved in the migratory process of cells. Hence, further study examined the role of SESN2 during the inhibition of cancer cell metastasis. First, scratch assays were conducted in HCT116 cells. After removal of cancer cells with scratch, treatments of 1% serum induced wound migration in Ad-LacZ-infected cells. However, the overexpression of SESN2 inhibited *in vitro* scratch wound migration (Fig. 11A). To confirm this, *in vitro* cancer cell migration and invasion assay were performed. Ad-LacZ-infected cells were significantly migrated cells in 10% serum-condition (Fig. 11B). However, Ad-SESN2 markedly repressed serum-induced *in vitro* cell migration (Fig. 11B). Next, *in vitro* cell invasion were examined by using matrigel coated invasion chamber in 10% serum-condition. Invasive population was increased in Ad-LacZ-infected cells, whereas infection of Ad-SESN2 notably suppressed serum-induced invaded cells (Fig. 11C). 5-FU treatment was used as positive control (Fig. 11B and 11C) to inhibit cell migration and invasion in colon cancer cells (Bogatkevich et al, 2008; Shen et al, 2014). These results support the notion that SESN2 inhibits cancer cell metastasis, which may result from ability of SESN2 to diminish HIF-1α level.

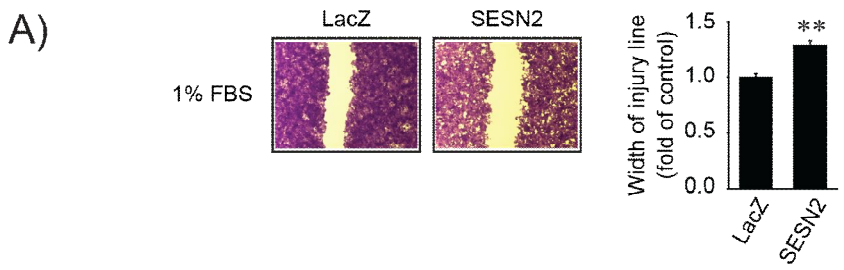

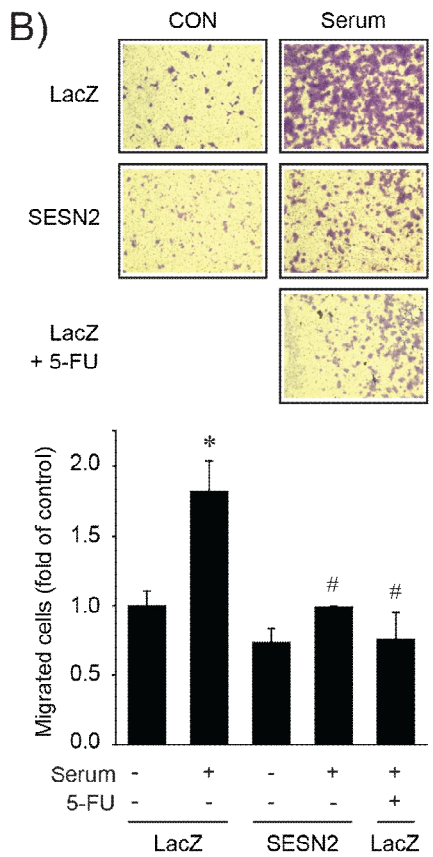

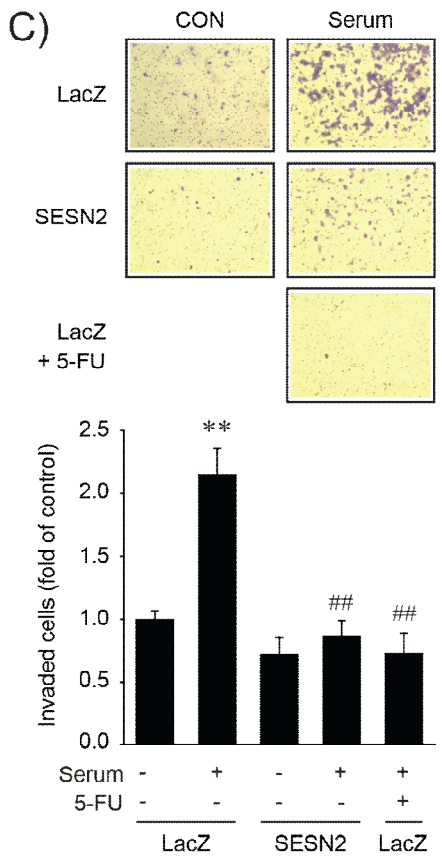

Fig. 11. Inhibition of *in vitro* cell migration and invasion by SESN2 overexpression

(A) Wound healing assay. HCT116 cells were seeded in 24-well plate following Ad-LacZ or Ad-SESN2 infection. Cells grown to 90% confluence were cleared with a scratch and then incubated with 1% serum for 24 h. Migrated cells were observed with light microscopy (magnification, ×50). The width of the injury line from three independent experiments was measured. The results presented were mean ± S.E.; $^{**}p < 0.01$ when compared to the Ad-LacZ-infected control.

(B) *In vitro* cell migration assay. HCT116 cells were placed in the upper part of the transwell plate following Ad-LacZ or Ad-SESN2 infection, and incubated with or without 10% serum for 24 h. 5-fluorouracil (5-FU, 50 μM) was used as positive control. Migrated cells were observed with light microscopy (magnification, ×100). The results shown are expressed as the mean ± S.E. from at least 3 different replicates; $^{*}p < 0.05$ when compared to the vehicle-treated control in Ad-LacZ-infected cells; $^{\#}p < 0.05$ when compared to the serum-treated Ad-LacZ-infected cells.

(C) *In vitro* cell invasion assay. HCT116 cells were placed in the upper part of the matrigel coted-transwell plate following Ad-LacZ or Ad-SESN2 infection, and incubated with or without 10% serum for 24 h. 5-FU (50 μM) was used as positive control. Invaded cells were observed with light microscopy (magnification, ×100). The results shown are expressed as the mean ± S.E. from at least 3 different replicates; $^{**}p < 0.01$ when compared to the vehicle-treated control in Ad-LacZ-infected cells; $^{\#\#}p < 0.01$ when compared to the serum-treated Ad-LacZ-infected cells.

4. Increase of ubiquitin-dependent HIF-1α degradation by SESN2 overexpression

Next study assessed the mRNA level of HIF-1α to see if changes in the level of HIF-1α mRNA precede that of protein by SESN2 overexpression. Treatment of $CoCl_2$ did not significantly affect the mRNA transcripts of HIF-1α in HCT116 cells. Moreover, when compared with Ad-GFP, Ad-SESN2 infection did not change the level of HIF-1α mRNA significantly (Fig. 12A). Treatment of actinomycin D, a transcription inhibitor, was adopted as a positive control, significantly decreased mRNA transcripts in compared to each control group (Fig. 12A); this result suggest that posttranscriptional mechanism possibly might be involved in SESN2-mediated HIF-1α regulation. In normoxia, HIF-1α is rapidly degraded by proteasome after ubiquitination via E3-ubiquitin ligase pVHL (Giaccia et al, 2003) and this pathway is recognized as the most important to regulate the level of HIF-1α. Therefore to find the molecular mechanism on inhibition of HIF-1α accumulation by SESN2, the stability of HIF-1α protein was examined. First, HIF-1α protein accumulation was induced by $CoCl_2$ treatment and then CHX (a protein translation inhibitor) was treated to observe and HIF-1α degradation. CHX treatment gradually showed decrease in accumulation of HIF-1α in both Ad-GFP and Ad-SESN2 infected cells (Fig. 12B). However, in the overexpression of SESN2, HIF-1α protein displayed a more decrease from 3 h after the start of the experiment and lower level at 60 min after treatment of CHX (Fig. 12B). To verify aforementioned results, cells were incubated with MG132, a proteasome inhibitor, and then cells were incubated under the condition of hypoxia or $CoCl_2$ treatment. After HIF-1α degradation was blocked by MG132 under hypoxia in HCT116 (Fig. 12C, left) and HT29 (Fig. 12C, right) cells, HIF-1α

ubiquitination was detected by immunoprecipitation assay. In the presence of MG132, Ad-SESN2 overexpression clearly increased HIF-1α-ubiquitination under hypoxic conditions in both HCT116 (Fig. 12C, left) and HT29 (Fig. 12C, right) cells. Moreover, Ad-SESN2 more facilitated ubiquitination of HIF-1α than Ad-GFP under both $CoCl_2$ and MG132 treatment in HCT116 (Fig. 12D, left) and HT29 (Fig. 12D, right) cells. These results clearly indicate that SESN2 promotes ubiquitination dependent proteasomal degradation of HIF-1α.

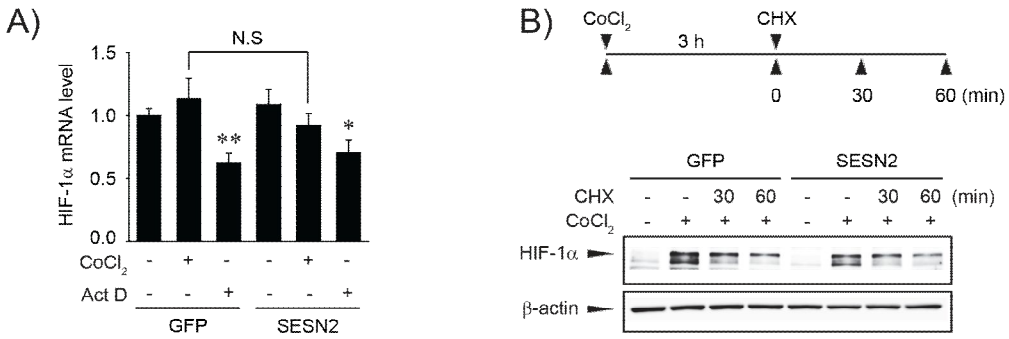

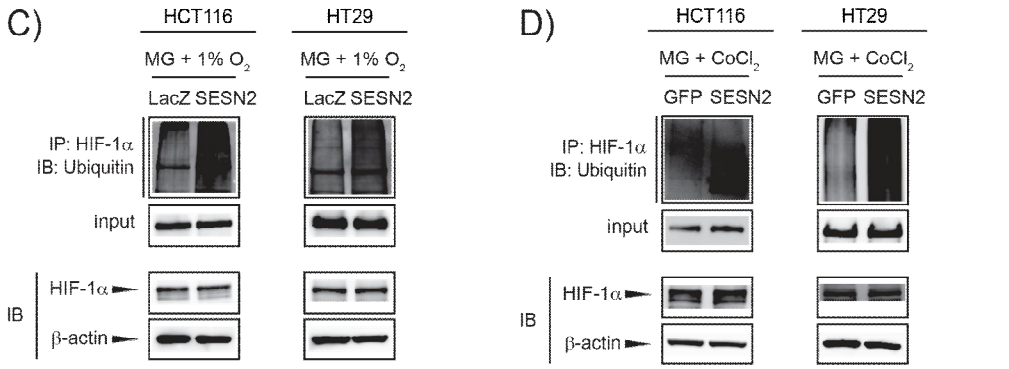

Fig. 12. Increase of ubiquitin-dependent HIF-1α degradation by SESN2 overexpression

(A) Real-time PCR assays. After Ad-GFP or Ad-SESN2 infection, HCT116 cells were pretreated with actinomycin D (Act D, 3 μg/mL) and then incubated with $CoCl_2$ (100 μM) for 6 h. Data were expressed as the mean ± S.E. from at least 3 different replicates; $^{*}p < 0.05$ or $^{**}p < 0.01$ when compared to the vehicle-treated Ad-GFP-or Ad-SESN2-infected cells.

(B) Immunoblot analysis. After Ad-GFP or Ad-SESN2 infection, HCT116 cells were incubated with $CoCl_2$ (100 μM) and cycloheximide (CHX, 0.5 μg/mL) for the indicated time periods. Lysates from these cells were then used to determine HIF-1α protein level via immunoblotting. These results show representative data of at least 3 separate experiments.

(C) Immunoprecipitation assay. After Ad-LacZ or Ad-SESN2 infection, HCT116 (left) or HT29 (right) cells that had been transfected with the plasmid encoding ubiquitin were pretreated with MG132 (MG, 10 μM) for 3 h and then incubated under the condition of hypoxia (1% oxygen) for 3 h. Immunoprecipitation assay was determined in the cell lysates. HIF-1α immunoprecipitates were immunoblotted with anti-ubiquitin antibody. HIF-1α and β-actin were immunoblotted in the cell lysates. These results show representative data of at least 3 separate experiments.

(D) Immunoprecipitation assay. After Ad-GFP or Ad-SESN2 infection, HCT116 (left) or HT29 (right) cells that had been transfected with the plasmid encoding ubiquitin were pretreated with MG (10 μM) for 3 h and then incubated in $CoCl_2$ (100 μM) for 6 h (left) or 3 h (right). Immunoprecipitation assay was determined in the cell lysates. HIF-1α immunoprecipitates were immunoblotted with anti-ubiquitin antibody. HIF-1α and β-actin were immunoblotted in the cell

lysates. These results show representative data of at least 3 separate experiments.

5. Involvement of PHD activation in SESN2-mediated inhibition of *in vitro* cell migration and invasion

To be degraded by the ubiquitination-proteasome system, the hydroxylation of proline residues (Pro402 and Pro564) in the oxygen-dependent degradation domain (ODDD) of HIF-1α by PHDs is a prerequisite (Kaelin Jr, 2008; Popovic et al, 2014). Next, to demonstrate whether SESN2 affects the hydroxylation of HIF-1α protein, hydroxyl-HIF-1α (OH-HIF-1α) level was examined. Hypoxia-induced OH-HIF-1α (Pro564) was increased for 3 h in Ad-LacZ-infected HCT116 (Fig. 13A, left) and HT29 (Fig. 13A, right) cells. When compared with the Ad-LacZ, Ad-SESN2 notably more increased the level of OH-HIF-1α in HCT116 (Fig. 13A, left) and HT29 (Fig. 13A, right) cells under hypoxia. But there was no difference the expression level of PHD2 between Ad-LacZ and Ad-SESN2 infected cells (Fig. 13A). Under $CoCl_2$ treatment, Ad-SESN2 also enhanced OH-HIF-1α in both colon cancer cells (Fig. 13B). These results suggest that SESN2 increases the level of HIF-1α hydroxlyation, thereby promoting HIF-1α degradation.

Next, to verify whether SESN2-induced increase of OH-HIF-1α affects on the cancer cell metastasis, cells were treated with DMOG, an inhibitor of PHD activity. The inhibitory effect on $CoCl_2$-induced HIF-1α accumulation by Ad-SESN2 was reversed by DMOG treatment in HCT116 cells (Fig. 14A). DMOG treatment notably repressed $CoCl_2$-induced hydroxylarion of HIF-1α in LacZ or SESN2 infected cells (Fig. 14A). This results indicates that hydroxylation of HIF-1α is a prerequisite for SESN2-mediated HIF-1α degradation. Next study examined the possibility that increase in hydroxylation of HIF-1α by SESN2 affects cancer cell metastasis. Consistent with aforementioned result, DMOG treatment abrogated the inhibitory effect of

10% serum-induced *in vitro* cell migration and invasion in Ad-SESN2 of HCT116 cells (Fig. 14B and 14C). These results show that SESN2-overexpressed cells increase PHD activity for HIF-1α hydroxylation, thereby preventing cancer cell migration and invasion.

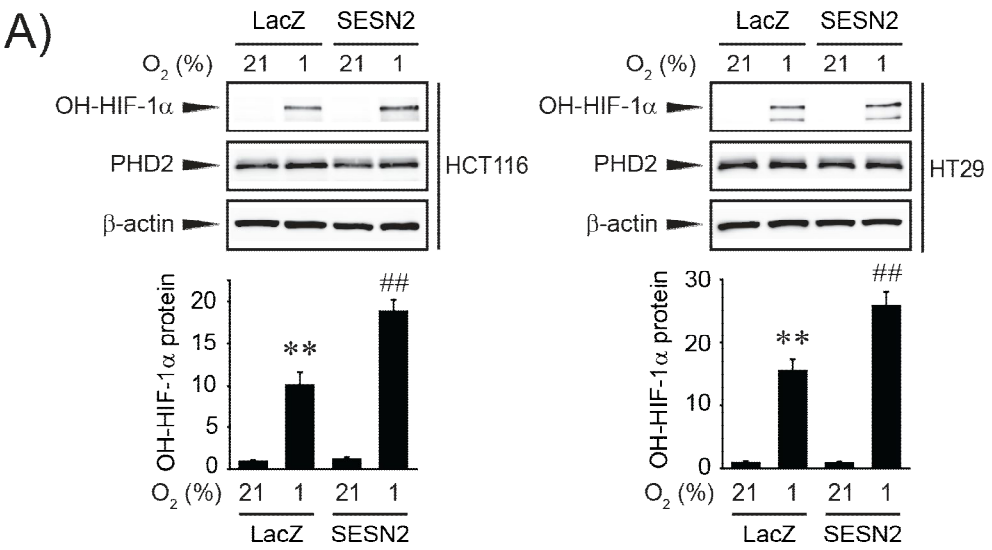

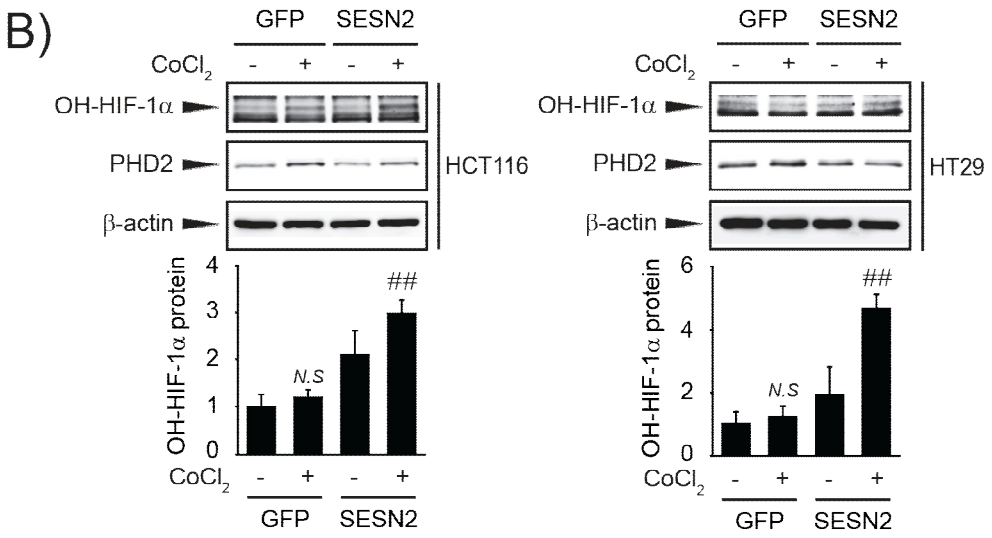

Fig. 13. The role of PHD activity in SESN2-mediated HIF-1α inhibition

(A) Immunoblot analysis. HCT116 (left) or HT29 (right) cells were incubated under the condition of normoxia (21% oxygen) or hypoxia (1% oxygen) for 3 h following Ad-LacZ or Ad-SESN2 infection. Lysates from these cells were then used to determine protein level via immunoblotting. The blots shown are expressed as the mean ± S.E. from at least 3 independent experiments; $^{**}p < 0.01$ when compared to the normoxia-incubated control in Ad-LacZ-infected cells; $^{\#\#}p < 0.01$ when compared to the hypoxia-incubated Ad-LacZ-infected cells.

(B) Immunoblot analysis. HCT116 (left) or HT29 (right) cells were incubated in $CoCl_2$ (100 μM) for 6 h (left) or 3 h (right) following Ad-LacZ or Ad-SESN2 infection. Lysates from these cells were then used to determine protein level via immunoblotting. The blots shown are expressed as the mean ± S.E. from at least 3 independent experiments; $^{\#\#}p < 0.01$ when compared to the $CoCl_2$-treated Ad-GFP-infected cells.

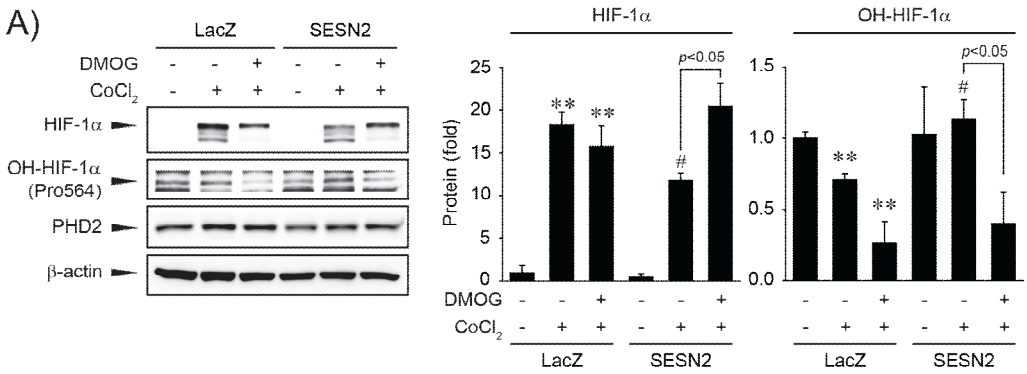

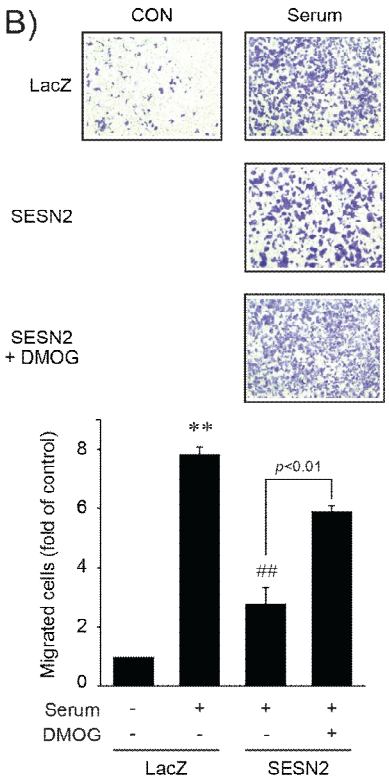

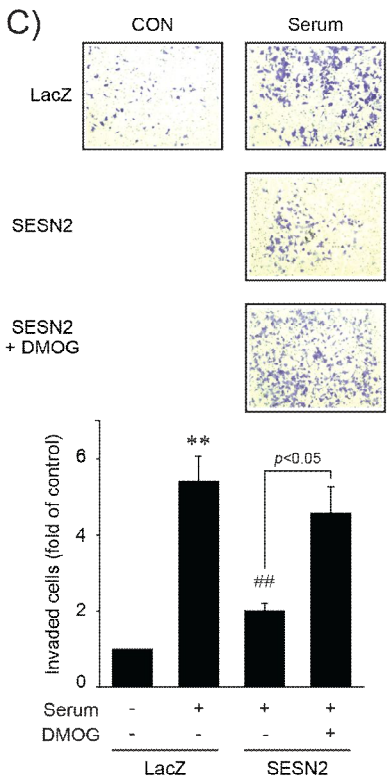

Fig. 14. Involvement of PHD activation in SESN2-mediated inhibition of *in vitro* cell migration and invasion

(A) Immunoblot analysis. After Ad-LacZ or Ad-SESN2 infection, HCT116 cells were pretreated with DMOG (1 mM) for 1 h and then incubated in $CoCl_2$ (100 μM) for 6 h. Lysates from these cells were then used to determine protein level via immunoblotting. The blots shown are expressed as the mean ± S.E. from at least 3 independent experiments; $^{**}p < 0.01$ when compared to the vehicle-treated control in Ad-LacZ-infected cells; $^{\#\#}p < 0.01$ when compared to the $CoCl_2$-treated Ad-LacZ-infected cells.

(B) *In vitro* cell migration assay. HCT116 cells were placed in the upper part of the transwell plate following Ad-LacZ or Ad-SESN2 infection, and treated with or without DMOG (1 mM) and continuously incubated with 10% serum for 24 h. Migrated cells were observed with light microscopy (magnification, ×100). The results shown are expressed as the mean ± S.E. from at least 3 different replicates; $^{**}p < 0.01$ when compared to the vehicle-treated control in Ad-LacZ-infected cells; $^{\#\#}p < 0.01$ when compared to the serum-treated Ad-LacZ-infected cells.

(C) *In vitro* cell invasion assay. HCT116 cells were placed in the upper part of the matrigel coted-transwell plate following Ad-LacZ or Ad-SESN2 infection, and treated with or without DMOG (1 mM) and continuously incubated with 10% serum for 24 h. Invaded cells were observed with light microscopy (magnification, ×100). The results shown are expressed as the mean ± S.E. from at least 3 different replicates; $^{**}p < 0.01$ when compared to the vehicle-treated control in Ad-LacZ-infected cells; $^{\#\#}p < 0.01$ when compared to the serum-treated Ad-LacZ-infected cells.

6. Inhibition of ROS-mediated HIF-1α accumulation by SESN2 overexpression

Previous study reported that excessive ROS production contributes to development of colorectal cancer (Waris and Ahsan, 2006). Moreover, generation of ROS in hypoxic condition leads to accumulate HIF-1α (Shimojo et al, 2013; Chandel et al, 2000; Goyal et al, 2004). Furthermore, prevention of oxidative stress improves tumor grade beneficially and inhibits metastasis (Sotgia et al, 2011). Based on the previous results that SESN2 is an antioxidant, next experiments explored whether the inhibitory effect of SESN2 on HIF-1α accumulation is related with its antioxidant capacity. To observe whether ROS production is involved in HIF-1α accumulation, the level of HIF-1α was assessed after H_2O_2 treatment. H_2O_2 significantly accumulated HIF-1α protein for 3–6 h in HCT116 (Fig. 15A, left) and for 1 h in HT29 (Fig. 15A, right) cells. H_2O_2-induced HIF-1α accumulation was also blocked by Ad-SESN2 in HCT116 and HT29 cells (Fig. 15A). In addition, measurement of ROS production using DCFH-DA indicated that Ad-SESN2 overexpression significantly inhibited increases in ROS production by $CoCl_2$ treatment (Fig. 15B). The antioxidant effect of SESN2 was verified by detection of H_2O_2-induced intracellular ROS generation (Fig. 15C). Therefore, the inhibition of HIF-1α accumulation by SESN2 may result from its antioxidant effect.

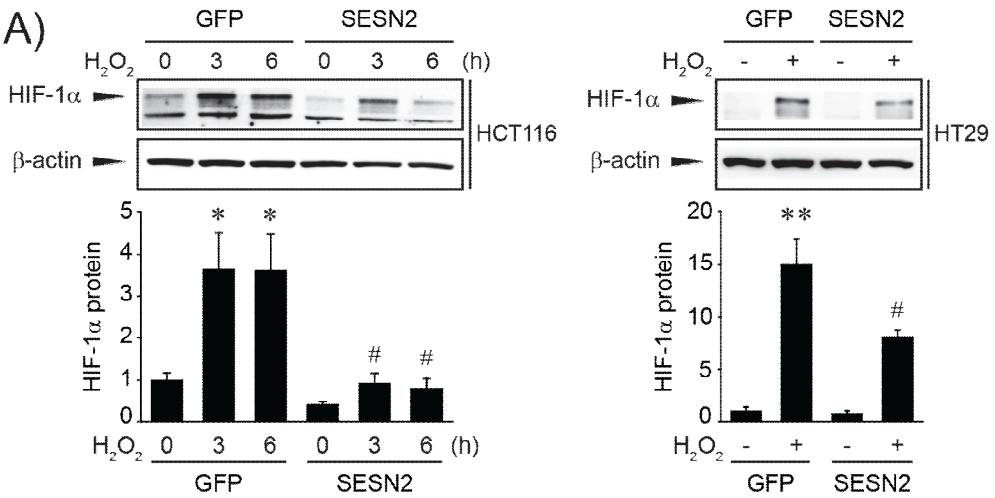

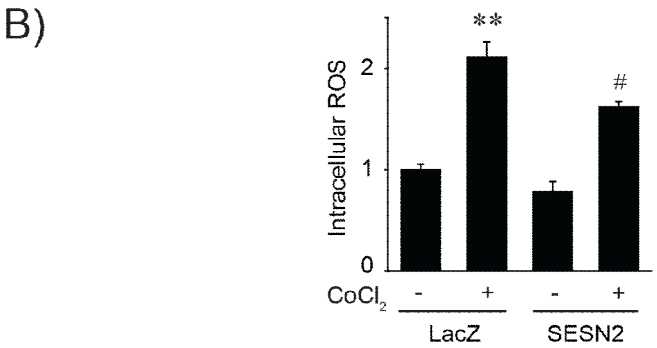

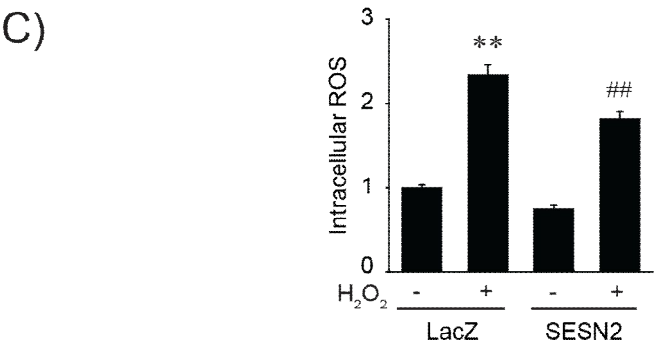

Fig. 15. Inhibition of ROS-mediated HIF-1α accumulation by SESN2 overexpression

(A) Immunoblot analysis. HCT116 (left) or HT29 (right) cells were exposed to H_2O_2 (500 μM) for 0–6 h (left) or 1 h (right) after Ad-GFP or Ad-SESN2 infection. Lysates from these cells were then used to determine protein level via immunoblotting. The blots shown are expressed as the mean ± S.E. from at least 3 independent experiments; $^{*}p < 0.05$ or $^{**}p < 0.01$ when compared to the vehicle-treated control in Ad-GFP-infected cells; $^{\#}p < 0.05$ when compared to the H_2O_2-treated Ad-GFP-infected cells.

(B) Measurement of ROS production. HCT116 cells were incubated with $CoCl_2$ (100 μM) for 30 min following Ad-LacZ or Ad-SESN2 infection. ROS production was assessed by DCF fluorescent intensity. Data represent the mean ± S.E. of data from at least 3 different replicates; $^{**}p < 0.01$ when compared to the vehicle-treated control in Ad-LacZ-infected cells; $^{\#}p < 0.05$ when compared to the $CoCl_2$-treated Ad-LacZ-infected cells.

(C) Measurement of ROS production. HCT116 cells were incubated with H_2O_2 (500 μM) for 10 min following Ad-LacZ or Ad-SESN2 infection. ROS production was assessed by DCF fluorescent intensity. Data represent the mean ± S.E. of data from at least 3 different replicates; $^{**}p < 0.01$ when compared to the vehicle-treated control in Ad-LacZ-infected cells; $^{\#\#}p < 0.01$ when compared to the H_2O_2-treated Ad-LacZ-infected cells.

7. The role of SESN2–AMPK axis in HIF-1α inhibition

AMPK plays a major role in maintaining energy and redox homeostasis in cells. Deregulation of this balance can lead to metabolic stress-associated disease (Steinberg and Kemp, 2009; Hardie, 2003; 2007; Hardie et al, 2012). AMPK activation inhibits HIF-1α accumulation (Lee et al, 2003; Jung et al, 2008; Treins et al, 2006). SESN2 has been documented as an upstream regulator of AMPK activation (Budanov and Karin, 2008; Ben-Sahra et al, 2013; Sanli et al, 2012). Therefore, to investigate the role of the SESN2–AMPK axis in HIF-1α inhibition, cells were transfected with an siRNA directed against human AMPKα. An siRNA knockdown of AMPKα reversed the Ad-SESN2-mediated inhibition of HIF-1α accumulation in HCT116 cells under hypoxia (Fig. 16A). Moreover, the increase of OH-HIF-1α by Ad-SESN2 under hypoxia was reversed by siRNA knockdown of AMPKα (Fig. 16A). This result showed that the possible role of AMPK signaling was required in the inhibitory action of Ad-SESN2 on HIF-1α destabilization. Similarly, a DN-AMPK to restore the ability of $CoCl_2$-induce HIF-1α accumulation against Ad-SESN2 (Fig. 16B, lower); DN-AMPK overexpression was confirmed by western blotting of AMPK truncated form (Fig. 16B, upper). The inhibitory effect of HRE luciferase activity under hypoxia in Ad-SESN2-overexpressing A549 cells was not seen in SESN2-overexpressing cells transfected with an siRNA knockdown (Fig. 16C, left); an siRNA knockdown of AMPKα was confirmed by immunoblot analysis (Fig. 16C, right). This result suggested that AMPK was responsible for SESN2-mediated inhibition of HIF-1α activity against hypoxia. These results indicate that repression HIF-1α accumulation by Ad-SESN2 may result from AMPK activation.

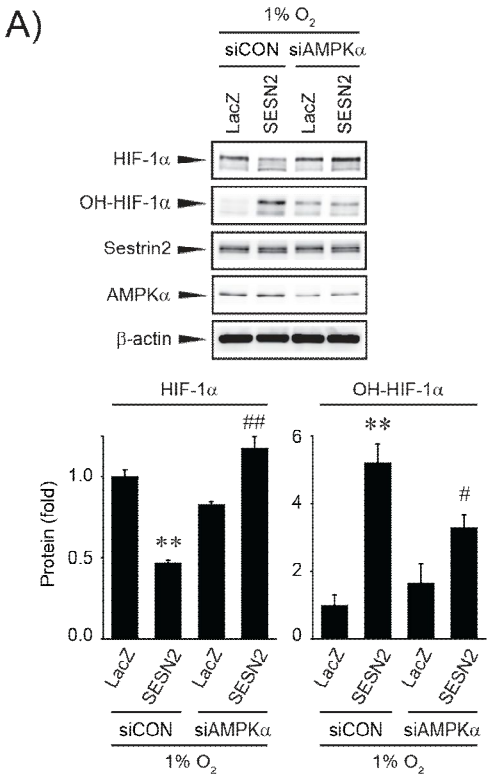

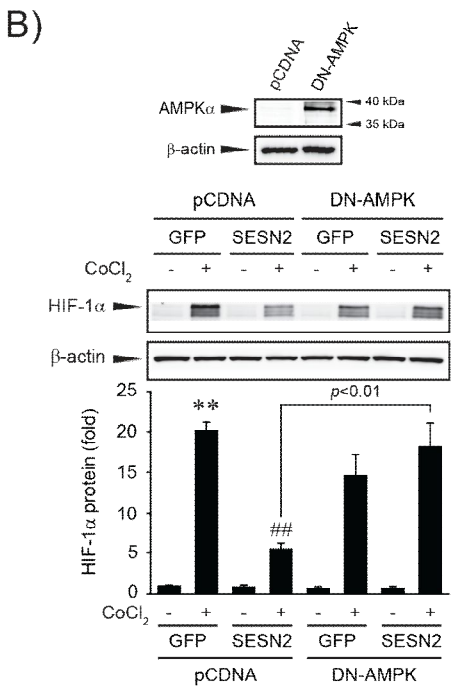

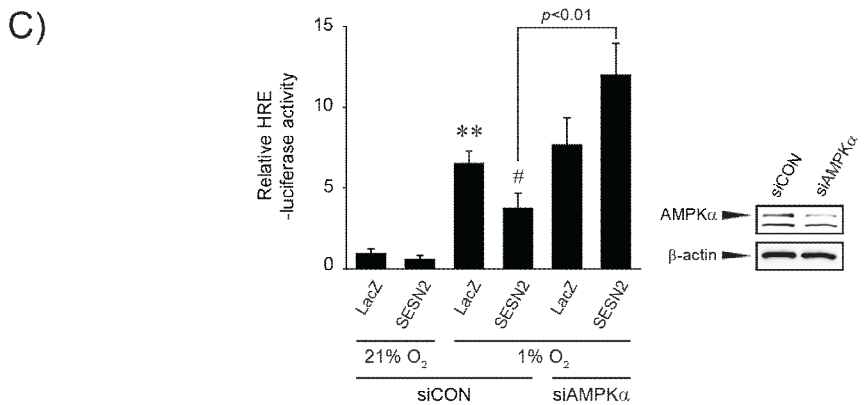

Fig. 16. The role of SESN2–AMPK axis in HIF-1α inhibition

(A) Immunoblot analysis. After Ad-LacZ or Ad-SESN2 infection, HCT116 cells were transfected with control siRNA (siCON) or AMPKα siRNA (siAMPKα). Then, HCT116 cells were incubated under the condition of hypoxia (1% oxygen) for 3 h. Lysates from these cells were then used to determine protein level via immunoblotting. The blots shown are expressed as the mean ± S.E. from at least 3 independent experiments; $^{**}p < 0.01$ when compared to the hypoxia-incubated control in Ad-LacZ-infected and siCON-transfected cells; $^{\#}p < 0.05$ or $^{\#\#}p < 0.01$ when compared to the hypoxia-incubated Ad-SESN2-infected and siCON-transfected cells.

(B) Immunoblot analysis. After Ad-GFP or Ad-SESN2 infection, HCT116 cells were transfected with a construct expressing a dominant-negative form of AMPK (DN-AMPK) or pCDNA. Then, cells were treated with $CoCl_2$ (100 μM) for 6 h. Protein levels were immunoblotted in the cell lysates. The blots shown are expressed as the mean ± S.E. from at least 3 independent experiments; $^{**}p < 0.01$ when compared to the vehicle-treated control in Ad-GFP-infected and pCDNA-transfected cells; $^{\#\#}p < 0.01$ when compared to the $CoCl_2$-treated Ad-GFP-infected and pCDNA-transfected cells.

(C) HRE reporter gene assay. After Ad-LacZ or Ad-SESN2 infection, HRE-A549 cells were transfected with siCON or siAMPKα. Then, HRE-A549 cells incubated under the condition of normoxia (21% oxygen) or hypoxia (1% oxygen) for 15 h. Luciferase activity was measured in the cell lysates. Data were expressed as the mean ± S.E. from at least 3 different replicates; $^{**}p < 0.01$ when compared to the normoxia-incubated control in Ad-LacZ-infected and siCON-transfected cells; $^{\#}p < 0.05$ when compared to the hypoxia-incubated Ad-LacZ-infected and siCON-transfected cells.

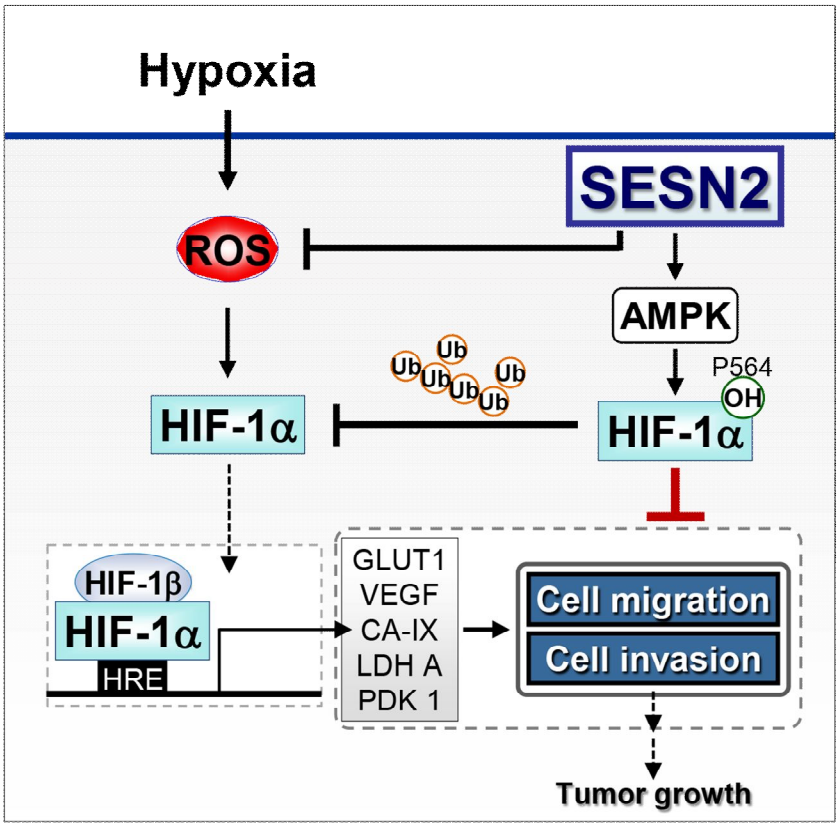

Fig. 17. Schematic diagram illustrating that SESN2 inhibits HIF-1α accumulation in hypoxia by increase of PHD activity and H_2O_2-scavenging effect

V. DISCUSSION

This study examines that SESN2 suppresses glucose deprivation-induced ROS production, thereby inhibiting mitochondrial dysfunction and apoptosis. In addition, SESN2 inhibits hypoxia-induced HIF-1α accumulation and cancer cell metastasis. This study also provides evidence that AMPK activation is required for the action of SESN2.

Family of SESNs (SESN1–3) has been discovered in mammals (Buckbinder et al, 1994; Budanov et al, 2002; Peeters et al, 2003). Although all isoforms of SESN have been documented to attenuate intracellular ROS, the each SESN induction is regulated by different mechanisms. The present study showed that glucose deprivation-induced SESN2 expression but not SESN1 in HepG2 cells (Fig. 1). Bae et al. also demonstrated that two diet states (fasting and refeeding) regulate SESN2 expression in mouse liver (Bae et al, 2013). In addition, *tert*-butyl hydroquinone leads to induction of SESN2 but not SESN1 or SESN3 (Shin et al, 2012) in HepG2 cells. Harmful environments such as gamma irradiation and genotoxic stress induce transcription of the SESN2 gene (Budanov et al, 2002; Velasco-Miguel et al, 1999). Hypoxia as one of the most severe metabolic condition also activates SESN2 gene transcription in human neuroblastoma cells (Budanov et al, 2002). Moreover, many compounds including 2-deoxyglucose which can decrease cellular ATP level, stimulates SESN2 expression (Ben-Sahra et al, 2013). Indeed, SESN2 is upregulated in obesity mouse tissue (liver and skeletal muscle) (Lee et al, 2012a). Collectively, these results suggest that especially SESN2 is sensitively induced in response to detrimental stimuli.

SESN2 participates in a variety of biological process, which protects function of diverse cells and tissues. It was shown that overexpressed SESN2 protects cells against oxidative

stress- and hypoxia-induced cell death (Budanov et al, 2002, 2004). In addition, Lee et al. reported that SESN2 prevents ROS overproduction thereby maintaining cellular metabolism and mitochondrial function (Lee et al, 2010b). In glomerular mesangial cells, it prevents hyperglycemia-induced dysfunction of endothelial nitric oxide synthase and fibronectin synthesis (Eid et al, 2013). Moreover, SESN2 also contributes to the inhibition of hepatic lipogenesis by the liver X receptor α (LXRα)-mediated SREBP-1c expression (Jin et al, 2013). In addition, this study shows that SESN2 protects mitochondrial function and increases cell survival against glucose depletion. Collectively, SESN2 has been shown to prevent stress-induced malfunction of cells.

ROS are important stimuli to induce SESN2. It is well known that ROS induce a lot of antioxidant genes via Nrf2-ARE activation (Lee et al, 2010a; Nguyen et al, 2009). SESN2 is also regulated by Nrf2-ARE dependent signal pathway (Shin et al, 2012). ROS induce Nrf2 phosphorylation, which results in separation Nrf2 from Kelch-like ECH-associated protein 1 (Keap1), an inhibitory regulator of Nrf2 (Itoh et al, 2004). This process increases Nrf2 stability and enables to translocate Nrf2 to nucleus (Itoh et al, 2004). Present study showed that glucose deprivation-induced Nrf2 phosphorylation at Serine 40 (Fig. 3A). In addition, this study found Nrf2-ARE activation-mediated SESN2 induction as evidence by measurement of SESN2 promoter activity (Fig. 3B). ΔARE in the region of the SESN2 promoter blocked the glucose deprivation-induced increase of SESN2 reporter activity (Fig. 3B). These observations suggest that the ARE region is involved in Nrf2-dependent induction of SESN2 gene.

This study focused on the protective effects of SESN2 is due to preserve mitochondrial function. Mitochondria membrane potential is important to produce ATP, therefore its loss mainly representative indicates of mitochondrial dysfunction and subsequently decreases the level of ATP (Green and Reed 1998). This study verified that overexpression of SESN2

prevented mitochondrial dysfunction, as supported by the decreased ADP/ATP ratio and recovery of mtDNA contents and mitochondrial membrane potential (Fig. 6). However, directly linkage between SESN2 and mitochondria has not been well defined. Based on AMPK is a downstream target of SESN2 and also plays a role in sensing ATP level, this study examined that the AMPK activation is involved in SESN2-mediated protection of mitochondrial damage. In response to an increase in the AMP/ATP ratio, AMPK represses ATP-consuming processes and increases ATP synthesis (Steinberg and Kemp, 2009). The recovery of mitochondria permeability transition elicited by SESN2 overexpression was reversed in DN-AMPK transfection (Fig. 7C). Moreover, treatment with AICAR prevented glucose deprivation-induced cell death (Fig. 7D); this result suggests that AMPK activation is responsible for SESN2-mediated protective effect of mitochondria and cell death against glucose deprivation. Since mitochondria are the sites of ATP production, mitochondria are probably target of AMPK to maintain cellular energy status (Steinberg and Kemp, 2009). Moreover, it is well established that AMPK represses accumulation of ROS in mitochondria through enhancing the mRNA level of peroxisome proliferators-activated response-coactivator-1, uncoupling protein, and MnSOD (Kukidome et al, 2006). Indeed, AMPK activation can preserve mitochondrial membrane permeability by suppressing glycogen synthase kinase 3β (GSK3β) (Shin et al, 2009). Oxidative stress is able to activate GSK3β, which in turn translocates into the mitochondria, finally, permeability transition pore is phosphorylation and membrane potential is break down; components phosphorylation is critical role in the mitochondrial permeability transition pore opening (Juhaszova et al, 2004; Xi et al, 2009). Therefore, the critical role of AMPK in inhibitory effect of GSK3β phosphorylation leads to protect on mitochondria. In addition, since SESN2 and AMPK are negative regulator of mTOR signaling (Lee et al, 2012a), ATP-consuming procedures by mTOR may be target of maintain

ATP levels in metabolic stress.

Hypoxia also affects the function of mitochondria. Normal cells metabolize glucose to pyruvate and then produce ATP through TCA cycle in mitochondria respiratory chain (Rudich et al, 2007). In mitochondria, OXPHOS system utilizes the proton gradient formed during electron flow from a reduced substrate to molecular oxygen to synthesize ATP from ADP (Rudich et al, 2007). Therefore, distribution of oxygen has been shown to be essential for preservation of mitochondrial function.

Unlike normal cells, tumor cells can generally adapt to and overcome hypoxia by diverse mechanisms including angiogenesis and switching glucose metabolism to glycolysis (Keith et al, 2012; Kleiner and Stetler-Stevenson, 1999; Liu et al, 2012; Parks et al, 2013). The adaptive response in hypoxia is primarily regulated by the transcription factor HIF-1α. Koop et al. documented that HIF-1a transactivates VEGF and plays a crucial role in angiogenesis and tumor formation (Koop et al, 2003). HIF-1 also stimulates glycolytic pathway by transactivating genes involved in extracellular glucose transport (such as GLUT1) and enzymes responsible for the glycolytic breakdown of intracellular glucose (such as Aldolase) (Chen et al, 2001; Semenza et al, 1994). In hypoxia, pyruvate is not used by mitochondria, instead it is converted to lactate by LDH to be released into the extracellular space, resulting in cancer cell acidosis (Firth et al, 1995). Moreover, CA-IX maintains cellular acidosis, thus, facilitates cancer cell growth and invasion (Semenza, 2003). Furthermore, HIF-1 also downregulates OXPHOS system within the mitochondria through PDK1 induction (Kim et al, 2006; Papandreou et al, 2006). Thus, HIF-1α is considered as a promising target against cancer progression and growth (Weidemann and Johnson, 2008; Yee et al, 2008).

SESN2 is originally reported as a p53 dependent gene (Budanov et al, 2002). SESN2 is frequently deleted in cancer (Velasco-Miguel et al, 1999) and SESN2 expression is especially

decreased in colorectal cancer (Wei et al, 2015). SESN2 represses cell growth and proliferation in many cancer cell lines (Budanov and Karin, 2008; Budanov et al, 2002). Moreover, silencing of both SESN2 and p53 promotes tumor growth in mice xenograft models (Sablina et al, 2005). However, effects of SESN2 on cancer metastasis, especially HIF-1α mediated process in hypoxia never have been explored. This study found that SESN2 represses serum-induced *in vitro* cell migration and invasion (Fig. 11). Moreover, its inhibitory effect was reversed by blockade of PHD activation (Fig. 14); support the concept that SESN2 may have inhibitory effects on tumor metastasis probably at least in part through PHD activation.

Hydroxylation of HIF-1α by PHD is necessarily required for proteasomal degradation (Kaelin Jr, 2008; Popovic et al, 2014). Therefore, regulation of PHD activity is recognized as important target for HIF-1α inhibition. Han et al. have documented that transforming growth factor-β1 increased HIF-1α accumulation via down-regulate PHD2 expression, thereby leading to epithelial-mesenchymal transition (EMT) in renal tubular cells (Han et al, 2013). In glioblastoma cells, PHD2 constitutively suppresses HIF-1α expression and regulates induction of HIF-1α-driven genes (Sun et al, 2014). In addition, PHD2 causes repression of pancreatic *in vivo* tumor growth and invasion (Su et al, 2012). Although how SESN2 regulates the interaction between PHD2 and HIF-1α is unclear, SESN2 increased HIF-1α hydroxylation (Fig. 13). These results imply that the PHD2 probably is an important downstream target of SESN2 in HIF-1α inhibition.

Present study provides evidence that SESN2 prevents the ability of hypoxia-induced ROS production and this process might contribute to inhibit HIF-1α accumulation and transactivation (Fig. 10 and 15). Accumulated reports have been indicated that antioxidants can inhibit HIF-1α accumulation and its action on cancer proliferation and metastasis (Lee et al,

2012b; Shimojo et al, 2013). Inhibition of ROS by NAC suppresses hypoxia-induced EMT and representative marker of metastasis in pancreatic cancers (Shimojo et al, 2013). Moreover, oltipraz (a cancer chemopreventive agent) promotes HIF-1α ubiquitin-dependent proteasomal degradation by its antioxidant effect (Lee et al, 2009b). Overall, SESN2 is likely to inhibit HIF-1α accumulation and adaptation of cancer cells to tumor microenvironments via repression of ROS production.

In addition, present study also suggests the role of AMPK in inhibition of HIF-1α accumulation by SESN2. An siRNA knockdown of AMPK or overexpression of DN-AMPK showed reversal inhibitory effect of SESN2 on HIF-1α accumulation (Fig. 16A and 16B). Previous report also indicated that AMPK activation by its activator AICAR or metformin antagonized insulin- or insulin-like growth factor-mediated HIF-1α accumulation, suggesting that AMPK activation can inhibit HIF-1α activation (Treins et al, 2006). Moreover, it has been known that hemin increased the GSK3β phosphorylation, therefore, either AMPK or GSK3 β might be link in the inhibition of HIF-1α (Lee et al, 2012b). Recently, Faubert et al. reported that the knockout of AMPKα accelerates the development of lymphomas in c-Myc-overexpressed transgenic mice, suggesting that loss of AMPK can contribute to promote tumor development (Faubert et al, 2013). In addition, AMPK has shown that tumor suppressor activity through HIF-1α and its target gene inhibition in mice (Faubert et al, 2013; 2015). In agreement with these previous reports, this study identified that siRNA knockdown of AMPK in Ad-SESN2 leads to reverse inhibition of HIF-1α activity (Fig. 16); this result corroborates AMPK signaling is involved in SESN2-mediated reduction of HIF-1α activation.

In conclusion, SESN2 shows wide-ranging influence on metabolic stress-induced adaptive response. This study provides that SESN2 prevents cellular damage associated with imbalance

of energy metabolism and inhibits HIF-1α mediated tumor metastasis. These findings strongly support novel insights into the crucial role of SESN2 in metabolic stress.

VI. CONCLUSION

1. Glucose deprivation induced SESN2 in hepatocyte-derived cells.
2. SESN2 decreased ROS production and apoptosis under glucose deprivation.
3. SESN2 restored the glucose deprivation-induced mitochondrial dysfunction.
4. AMPK activation was responsible for SESN2-mediated mitochondrial protection against glucose deprivation.
5. SESN2 repressed the serum-induced *in vitro* cancer cell migration and invasion.
6. SESN2 decreased ROS-mediated HIF-1α accumulation in colorectal cancer cells.
7. SESN2 increased HIF-1α hydroxylation thereby promoting ubiquitin-dependent HIF-1α degradation.
8. AMPK activation was responsible for SESN2-mediated effect of HIF-1α destabilization.

REFERENCES

Ahmad, I. M.; Aykin-Burns, N.; Sim, J. E.; Walsh, S. A.; Higashikubo, R.; Buettner, G. R.; Venkataraman, S.; Mackey, M. A.; Flanagan, S. W.; Oberley, L. W.; Spitz, D. R. Mitochondrial O_2^- and H_2O_2 mediate glucose deprivation-induced stress in human cancer cells. *J. Biol. Chem.* **280:**4254-4263; 2005.

Argyrou, A.; Blanchard, J. S. Flavoprotein disulfide reductases: advances in chemistry and function. *Prog. Nucleic Acid Res. Mol. Biol.* **78:**89-142; 2004.

Bae, S. H.; Sung, S. H.; Oh, S. Y.; Lim, J. M.; Lee, S. K.; Park, Y. N.; Lee, H. E.; Kang, D.; Rhee, S. G. Sestrins activate Nrf2 by promoting p62-dependent autophagic degradation of Keap1 and prevent oxidative liver damage. *Cell Metab.* **17:**73-84; 2013.

Ben-Sahra, I.; Dirat, B.; Laurent, K.; Puissant, A.; Auberger, P.; Budanov, A.; Tanti, J. F.; Bost, F. Sestrin2 integrates Akt and mTOR signaling to protect cells against energetic stress-induced death. *Cell Death Differ.* **20:**611-619; 2013.

Biteau, B.; Labarre, J.; Toledano, M. B. ATP-dependent reduction of cysteinesulphinic acid by S. cerevisiae sulphiredoxin. *Nature* **425:**980-984; 2003.

Blackburn, R. V.; Spitz, D. R.; Liu, X.; Galoforo, S. S.; Sim, J. E.; Ridnour, L. A.; Chen, J. C.; Davis, B. H.; Corry, P. M.; Lee, Y. J. Metabolic oxidative stress activates signal transduction and gene expression during glucose deprivation in human tumor cells. *Free Radic. Biol. Med.* **26:**419-430: 1999.

Blumberg, J. Use of biomarkers of oxidative stress in research studies. *J. Nutr.* **134:**3188S-3189S; 2004.

Bogatkevich, G. S.; Ludwicka-Bradley, A.; Singleton, C. B.; Bethard, J. R.; Silver, R. M.

Proteomic analysis of CTGF-activated lung fibroblasts: identification of IQGAP1 as a key player in lung fibroblast migration. *Am. J. Physiol. Lung. Cell Mol. Physiol.* **295:**L603-L611; 2008.

Borren, A.; Groenendaal, G.; van der Groep, P.; Moman, M. R.; Boeken Kruger, A. E.; van der Heide, U. A.; Jonges, T. N.; van Diest, P. J.; van Vulpen, M.; Philippens, M. E. Expression of hypoxia-inducible factor-1α and -2α in whole-mount prostate histology: relation with dynamic contrast-enhanced MRI and Gleason score. *Oncol. Rep.* **29:**2249-2254; 2013.

Brown, G. C.; Borutaite, V. Nitric Oxide, Mitochondria, and Cell Death. *IUBMB Life* **52:**189-195; 2001.

Buckbinder, L.; Talbott, R.; Seizinger, B. R.; Kley, N. Gene regulation by temperature-sensitive p53 mutants: identification of p53 response genes. *Proc. Natl. Acad. Sci. USA.* **91:**10640-10644; 1994.

Budanov, A. V.; Karin, M. p53 Target genes Sestrin1 and Sestrin2 connect genotoxic stress and mTOR signaling. *Cell* **134:**451-460; 2008.

Budanov, A. V.; Lee, J. H.; Karin, M. Stressin' Sestrins take an aging fight. *EMBO Mol. Med.* **2:**388-400; 2010.

Budanov, A. V.; Sablina, A. A.; Feinstein, E.; Koonin, E. V.; Chumakov, P. M. Regeneration of peroxiredoxins by p53-regulated Sestrins, homologs of bacterial AhpD. *Science* **304:**596-600; 2004.

Budanov, A. V.; Shoshani, T.; Faerman, A.; Zelin, E.; Kamer, I.; Kalinski, H.; Gorodin, S.; Fishman, A.; Chajut, A.; Einat, P.; Skaliter, R.; Gudkov, A. V.; Chumakov, P. M.; Feinstein, E. Identification of a novel stress-responsive gene Hi95 involved in regulation of cell viability. *Oncogene* **21:**6017-6031; 2002.

Cadenas, E.; Davies, K. J. A. Mitochondrial free radical generation, oxidative stress, and aging. *Free Radic. Biol. Med.* **29:**222-230; 2000.

Chandel, N. S.; McClintock, D. S.; Feliciano, C. E.; Wood, T. M.; Melendez, J. A.; Rodriguez, A. M.; Schumacker, P. T. Reactive oxygen species generated at mitochondrial complex III stabilize hypoxia-inducible factor-1alpha during hypoxia: a mechanism of O_2 sensing. *J. Biol. Chem.* **275:**25130-25138; 2000.

Chang, T. S.; Jeong, W.; Woo, H. A.; Lee, S. M.; Park, S.; Rhee, S. G. Characterization of mammalian sulfiredoxin and its reactivation of hyperoxidized peroxiredoxin through reduction of cysteine sulfinic acid in the active site to cysteine. *J. Biol. Chem.* **279:**50994-51001; 2004.

Chen, C.; Pore, N.; Behrooz, A.; Ismail-Beigi, F.; Maity. A. Regulation of glut1 mRNA by hypoxia-inducible factor-1. Interaction between H-ras and hypoxia. *J. Biol. Chem.* **276:**9519-9525; 2001.

Chen, Y. -S.; Chen, S. -D.; Wu, C. -L.; Huang, S. -S.; Yang, D. -I. Induction of Sestrin2 as an endogenous protective mechanism against amyloid beta-peptide neurotoxicity in primary cortical culture. *Exp. Neurol.* **253:**63-71; 2014.

Codoñer-Franch, P.; Navarro-Ruiz, A.; Fernández-Ferri, M.; Arilla-Codoñer, A.; Ballester-Asensio, E.; Valls-Bellés, V. A matter of fat: insulin resistance and oxidative stress. *Pediatr. Diabetes* **13:**392-399; 2012.

D'Autréaux, B.; Toledano, M. B. ROS as signalling molecules: mechanisms that generate specificity in ROS homeostasis. Nat. Rev. Mol. Cell Biol. **8:**813-824; 2007.

D'Autréaux, B.; Toledano, M. B. ROS as signalling molecules: mechanisms that generate specificity in ROS homeostasis. *Nat. Rev. Mol. Cell. Biol.* **8:**813-824; 2007.

De Saedeleer, C. J.; Porporato, P. E.; Copetti, T.; Pérez-Escuredo, J.; Payen, V. L.; Brisson, L.;

Feron, O.; Sonveaux, P. Glucose deprivation increases monocarboxylate transporter 1 (MCT1) expression and MCT1-dependent tumor cell migration. *Oncogene* **33:**4060-4068; 2014.

Deisseroth, A.; Dounce, A. L. Catalase: Physical and chemical properties, mechanism of catalysis, and physiological role. *Physiol. Rev.* **50:**319-375; 1970.

Denko, N. C. Hypoxia, HIF1 and glucose metabolism in the solid tumour. *Nat. Rev. Cancer* **8:**705-713; 2008.

DiMauro, S.; Schon, E. A. Mitochondrial respiratory-chain diseases. *N. Engl. J. Med.* **348:**2656-2668; 2003.

Drummond, G. R.; Selemidis, S.; Griendling, K. K.; Sobey, C. G. Combating oxidative stress in vascular disease: NADPH oxidases as therapeutic targets. *Nat. Rev. Drug Discov.* **10:**453-471; 2011.

Eid, A. A.; Lee, D.-Y.; Roman, L. J.; Khazim, K.; Gorin, Y. Sestrin 2 and AMPK connect hyperglycemia to Nox4-dependent endothelial nitric oxide synthase uncoupling and matrix protein expression. *Mol. Cell. Biol.* **33:**3439-3460; 2013.

Essler, S.; Dehne, N.; Brune, B. Role of Sestrin2 in peroxide signaling in macrophages. *FEBS Lett.* **583:**3531-3535; 2009.

Faubert, B.; Boily, G.; Izreig, S.; Griss, T.; Samborska, B.; Dong, Z.; et al. AMPK is a negative regulator of the Warburg effect and suppresses tumor growth *in vivo*. *Cell Metab.* **17:**113-124; 2013.

Faubert, B.; Vincent, E. E.; Poffenberger, M. C.; Jones, R. G. The amp-activated protein kinase (ampk) and cancer: many faces of a metabolic regulator. *Cancer Lett.* **356:**165-170; 2015.

Finkel, T. Oxidant signals and oxidative stress. *Curr. Opin. Cell Biol.* **15:**247-254; 2003.

Firth, J. D.; Ebert, B. L.; Ratcliffe, P. J. Hypoxic regulation of lactate dehydrogenase A.

Interaction between hypoxia-inducible factor 1 and cAMP response elements. *J. Biol. Chem.* **270:**21021-21027; 1995.

Forman, H. J.; Fridovich, I. Superoxide dismutase: a comparison of rate constants. *Arch. Biochem. Biophys.* **158:**396-400; 1973.

Furukawa, S.; Fujita, T.; Shimabukuro, M.; Iwaki, M.; Yamada, Y.; Nakajima, Y.; Nakayama, O.; Makishima, M.; Matsuda, M.; Shimomura, I. Increased oxidative stress in obesity and its impact on metabolic syndrome. *J. Clin. Invest.* **114:**1752-1761; 2004.

Giaccia, A.; Siim, B. G.; Johnson, R. S. HIF-1 as a target for drug development. *Nat. Rev. Drug Discov.* **2:**803-811; 2003.

Gnaiger, E.; Méndez, G.; Hand, S. C. High phosphorylation efficiency and depression of uncoupled respiration in mitochondria under hypoxia. *Proc. Natl. Acad. Sci. USA.* **97:**11080-11085; 2000.

Go, Y. M.; Jones, D. P. Redox control systems in the nucleus: mechanisms and functions. *Antioxid. Redox. Signal.* **13:**489-509; 2010.

Gossage, L., Eisen, T., Maher, E. R. VHL, the story of a tumour suppressor gene. *Nat. Rev. Cancer.* **15:**55-64; 2015.

Goyal, P.; Weissmann, N.; Grimminger, F.; Hegel, C.; Bader, L.; Rose, F.; Fink, L.; Ghofrani, H. A.; Schermuly, R. T.; Schmidt, H. H.; Seeger, W.; Hänze, J. Upregulation of NAD(P)H oxidase 1 in hypoxia activates hypoxia-inducible factor 1 via increase in reactive oxygen species. *Free Radic. Biol. Med.* **36:**1279-1288; 2004.

Green, D. R.; Reed, J. C. Mitochondria and apoptosis. *Science* **281:**1309-1312; 1998.

Gwinn, D. M.; Shackelford, D. B.; Egan, D. F.; Mihaylova, M. M.; Mery, A.; Vasquez, D. S.; Turk, B. E.; Shaw, R. J. AMPK phosphorylation of raptor mediates a metabolic checkpoint. *Mol. Cell* **30:**214-226; 2008.

Han, W. Q.; Zhu, Q.; Hu, J.; Li, P. L.; Zhang, F.; Li, N. Hypoxia-inducible factor prolyl-hydroxylase-2 mediates transforming growth factor beta 1-induced epithelial–mesenchymal transition in renal tubular cells. *Biochim. Biophys. Acta.* **1833:**1454-1462; 2013.

Handy, D. E.; Loscalzo, J. Redox regulation of mitochondrial function. *Antioxid. Redox Signal.* **16:**132313-132367; 2012.

Hardie, D. G. AMP-activated/SNF1 protein kinases: conserved guardians of cellular energy. *Nat. Rev. Mol. Cell Biol.* **8:**774-785; 2007.

Hardie, D. G.; Ross, F. A.; Hawley, S. A. AMPK: a nutrient and energy sensor that maintains energy homeostasis. *Nat. Rev. Mol. Cell Biol.* **13:**251-262; 2012.

Hardie, D. G.; Scott, J. W.; Pan, D. A.; Hudson, E. R. Management of cellular energy by the AMP-activated protein kinase system. *FEBS Lett.* **546:**113-120; 2003.

Hermsdorff, H. H.; Barbosa, K. B.; Volp, A. C.; Puchau, B.; Bressan, J.; Zulet, M. Á.; Martínez, J. A. Gender-specific relationships between plasma oxidized low-density lipoprotein cholesterol, total antioxidant capacity, and central adiposity indicators. *Eur. J. Prev. Cardiol.* **21:**884-891; 2014.

Hermsdorff, H. H.; Volp, A. C.; Puchau, B.; Barbosa, K. B.; Zulet, M. A.; Bressan, J.; Martínez, J. A. Contribution of gender and body fat distribution to inflammatory marker concentrations in apparently healthy young adults. *Inflamm. Res.* **61:**427-435; 2012.

Hunter, D. R.; Haworth, R. A.; Southard, J. H. Relationship between configuration, function, and permeability in calcium-treated mitochondria. *J. Biol. Chem.* **251:**5069-5077; 1976.

Hwahng, S. H.; Ki, S. H.; Bae, E. J.; Kim, H. E.; Kim, S. G. Role of adenosine monophosphate-activated protein kinase–p70 ribosomal S6 kinase-1 pathway in repression of liver X receptor-alpha–dependent lipogenic gene induction and hepatic steatosis by a novel class

of dithiolethiones. *Hepatology* **49:**1913-1925; 2009.

Ido, Y.; Carling, D.; Ruderman, N. Hyperglycemia-Induced Apoptosis in Human Umbilical Vein Endothelial Cells Inhibition by the AMP-Activated Protein Kinase Activation. *Diabetes* **51:**159-167; 2002.

Imlay, J. A. Pathways of oxidative damage. *Annu. Rev. Microbiol.* **57:**395-418; 2003.

Itoh, K.; Tong, K. I.; Yamamoto, M. Molecular mechanism activating Nrf2–keap1 pathway in regulation of adaptive response to electrophiles. *Free Radic. Biol. Med.* **36:**1208-1213; 2004.

Jaakkola, P.; Mole, D. R.; Tian, Y. M.; Wilson, M. I.; Gielbert, J.; Gaskell, S. J.; von Kriegsheim, A.; Hebestreit, H. F.; Mukherji, M.; Schofield, C. J.; Maxwell, P. H.; Pugh, C. W.; Ratcliffe, P. J. Targeting of HIF-alpha to the von Hippel-Lindau ubiquitylation complex by O_2-regulated prolyl hydroxylation. *Science* **292:**468-472; 2001.

Jin, S. H.; Yang, J. H.; Shin, B. Y.; Seo, K.; Shin, S. M.; Cho, I. J.; Ki, S. H. Resveratrol inhibits LXRα-dependent hepatic lipogenesis through novel antioxidant Sestrin2 gene induction. *Toxicol. Appl. Pharmacol.* **271:**95-105; 2013.

Jones, D. P. Intracellular diffusion gradients of O2 and ATP. *Am. J. Physiol.* **250:**C663-C675; 1986.

Jones, D. P. Radical-free biology of oxidative stress. *Am. J. Physiol. Cell Physiol.* **295:**C849-C868; 2008.

Juhaszova, M.; Zorov, D. B.; Kim, S.-H.; Pepe, S.; Fu, Q.; Fishbein, K. W.; Ziman, B. D.; Wang, S.; Ytrehus, K.; Antos, C. L.; Olson, E. N.; Sollott, S. J. Glycogen synthase kinase-3β mediates convergence of protection signaling to inhibit the mitochondrial permeability transition pore. *J. Clin. Invest.* **113:**1535-1549; 2004.

Jung, S. N.; Yang, W. K.; Kim, J.; Kim, H. S.; Kim, E. J.; Yun, H.; Park, H.; Kim, S. S.; Choe,

W.; Kang, I.; Ha, J. Reactive oxygen species stabilize hypoxia-inducible factor-1α protein and stimulate transcriptional activity via AMP-activated protein kinase in DU145 human prostate cancer cells. *Carcinogenesis* **29:**713-721; 2008.

Kadenbach, B.; Hüttemann, M. The subunit composition and function of mammalian cytochrome c oxidase. *Mitochondrion* **24:**64-76; 2015.

Kaelin, W. G. Jr. The von Hippel-Lindau tumour suppressor protein: O2 sensing and cancer. *Nat. Rev. Cancer* **8:**865-873; 2008.

Ke, Q.; Costa, M. Hypoxia-inducible factor-1 (HIF-1). *Mol. Pharmacol.* **70:**1469-1480; 2006.

Keith, B., Johnson, R. S., Simon, M. C. HIF1α and HIF2α: sibling rivalry in hypoxic tumour growth and progression. *Nat. Rev. Cancer* **12:**9-22; 2012.

Kim, J. S.; He, L.; Lemasters, J. J. Mitochondrial permeability transition: a common pathway to necrosis and apoptosis. *Biochem. Biophys. Res. Commun.* **304:**463-470; 2003.

Kim, J. W.; Tchernyshyov, I.; Semenza, G. L.; Dang, C. V. HIF-1-mediated expression of pyruvate dehydrogenase kinase: a metabolic switch required for cellular adaptation to hypoxia. *Cell. Metab.* **3:**177-185; 2006.

Kim, J. W.; Tchernyshyov, I.; Semenza, G. L.; Dang, C. V. HIF-1-mediated expression of pyruvate dehydrogenase kinase: a metabolic switch required for cellular adaptation to hypoxia. *Cell Metab.* **3:**177-185; 2006.

Kleiner, D. E.; Stetler-Stevenson, W. G. Matrix metalloproteinases and metastasis. *Cancer Chemother. Pharmacol.* **43:**S42-S51; 1999.

Kondo, T.; Ishida, Y. Molecular pathology of wound healing. *Forensic. Sci. Int.* **203:**93-98; 2010.

Koop, E. A.; Lopes, S. M.; Feiken, E.; Bluyssen, H. A.; van der Valk, M.; Voest, E. E.; Mummery, C. L.; Moolenaar, W. H.; Gebbink, M. F. Receptor protein tyrosine

phosphatase mu expression as a marker for endothelial cell heterogeneity; analysis of RPTPmu gene expression using LacZ knock-in mice. *Int. J. Dev. Biol.* **47:**345-354; 2003.

Kroemer, G.; Reed, J. C. Mitochondrial control of cell death. *Nat. Med.* **6:**513-519; 2000.

Kukidome, D.; Nishikawa, T.; Sonoda, K.; Imoto, K.; Fujisawa, K.; Yano, M.; Motoshima, H.; Taguchi, T.; Matsumura, T.; Araki, E. Activation of AMP-activated protein kinase reduces hyperglycemia-induced mitochondrial reactive oxygen species production and promotes mitochondrial biogenesis in human umbilical vein endothelial cells. *Diabetes* **55:**120-127; 2006.

Lee, H. G.; Li, M. H.; Joung, E. J.; Na, H. K.; Cha, Y. N.; Surh, Y. J. Nrf2-Mediated heme oxygenase-1 upregulation as adaptive survival response to glucose deprivation-induced apoptosis in HepG2 cells. *Antioxid. Redox Signal.* **13:**1639-1648; 2010a.

Lee, H.; Lee, Y. J.; Choi, H.; Ko, E. H.; Kim, J. W. Reactive oxygen species facilitate adipocyte differentiation by accelerating mitotic clonal expansion. *J. Biol. Chem.* **284:**10601-10609; 2009a.

Lee, J. H.; Budanov, A. V.; Park, E. J.; Birse, R.; Kim, T. E.; Perkins, G. A.; Ocorr, K.; Ellisman, M. H.; Bodmer, R.; Bier, E.; Karin, M. Sestrin as a feedback inhibitor of TOR that prevents age-related pathologies. *Science* **327:**1223-1228; 2010b.

Lee, J. H.; Budanov, A. V.; Talukdar, S.; Park, E. J.; Park, H. L.; Park, H. W.; Bandyopadhyay, G.; Li, N.; Aghajan, M.; Jang, I.; Wolfe, A. M.; Perkins, G. A.; Ellisman, M. H.; Bier, E.; Scadeng, M.; Foretz, M.; Viollet, B.; Olefsky, J.; Karin, M. Maintenance of metabolic homeostasis by Sestrin2 and Sestrin3. *Cell Metab*. **16:**311-321; 2012a.

Lee, J. H.; Budanov, Andrei, V.; Karin, M. Sestrins orchestrate cellular metabolism to attenuate aging. *Cell Metab.* **18:**792-801; 2013.

Lee, J. M.; Lee, W. H.; Kay, H. Y.; Kim, E. S.; Moon, A.; Kim, S. G. Hemin, an iron-binding

porphyrin, inhibits HIF-1α induction through its binding with heat shock protein 90. *Int. J. Cancer* **130:**716-727; 2012b.

Lee, M.; Hwang, J. T.; Lee, H. J.; Jung, S. N.; Kang, I.; Chi, S. G.; Kim, S. S.; Ha, J. AMP-activated protein kinase activity is critical for hypoxia-inducible factor-1 transcriptional activity and its target gene expression under hypoxic conditions in DU145 cells. *J. Biol. Chem.* **278:**39653-39661; 2003.

Lee, W. H.; Kim, Y. W.; Choi, J. H.; Brooks, S. C. 3rd.; Lee, M. O.; Kim, S. G. Oltipraz and dithiolethione congeners inhibit hypoxia-inducible factor-1alpha activity through p70 ribosomal S6 kinase-1 inhibition and H_2O_2-scavenging effect. *Mol. Cancer Ther.* **8:**2791-2802; 2009b.

Lemasters, J. J.; Nieminen, A. L. Mitochondrial oxygen radical formation during reductive and oxidative stress to intact hepatocytes. *Bioscience Rep.* **17:**281-291; 1997.

Lemasters, J. J.; Nieminen, A. L.; Qian, T.; Trost, L. C.; Elmore, S. P.; Nishimura, Y.; Crowe, R. A.; Cascio, W. E.; Bradham, C. A.; Brenner, D. A.; Herman, B. The mitochondrial permeability transition in cell death: a common mechanism in necrosis, apoptosis and autophagy. *Biochim. Biophys. Acta.* **1366:**177-196; 1998.

Lim, J. C.; Choi, H. I.; Park, Y. S.; Nam, H. W.; Woo, H. A.;, Kwon, K. S.; Kim, Y. S.; Rhee, S. G.; Kim, K.; Chae, H. Z. Irreversible oxidation of the active-site cysteine of peroxiredoxin to cysteine sulfonic acid for enhanced molecular chaperone activity. *J. Biol. Chem.* **283:**28873-28880; 2008.

Liu, F.; Lou, Y. L.; Wu, J.; Ruan, Q. F.; Xie, A.; Guo, F.; Cui, S. P.; Deng, Z. F.; Wang, Y. Upregulation of microRNA-210 regulates renal angiogenesis mediated by activation of VEGF signaling pathway under ischemia/perfusion injury *in vivo* and *in vitro*. *Kidney Blood Press Res.* **35:**182-191; 2012.

Lum, J. J.; Bui, T.; Gruber, M.; Gordan, J. D.; DeBerardinis, R. J.; Covello, K. L.; Simon, M. C.; Thompson, C. B. The transcription factor HIF-1α plays a critical role in the growth factor-dependent regulation of both aerobic and anaerobic glycolysis. *Genes Dev.* **21:**1037-1049; 2007.

Martindale, J. L.; Holbrook, N. J. Cellular response to oxidative stress: Signaling for suicide and survival. J. Cell. Physiol. **192:**1-15; 2002.

Métivier, D.; Dallaporta, B.; Zamzami, N.; Larochette, N.; Susin, S. A.; Marzo, I.; Kroemer, G. Cytofluorometric detection of mitochondrial alterations in early CD95/Fas/APO-1-triggered apoptosis of Jurkat T lymphoma cells. Comparison of seven mitochondrion-specific fluorochromes. *Immunol. Lett.* **61:**157-163; 1998.

Moley, K. H.; Mueckler, M. M. Glucose transport and apoptosis. *Apoptosis* **5:**99-105; 2000.

Nguyen, T.; Nioi, P.; Pickett, C. B. The Nrf2-antioxidant response element signaling pathway and its activation by oxidative stress. *J. Biol. Chem.* **284:**13291-13295; 2009.

Nicotera, P.; Leist, M.; Ferrando-May, E. Intracellular ATP, a switch in the decision between apoptosis and necrosis. *Toxicol. Lett.* **102-103:**139-142; 1998.

Niture, S. K.; Khatri, R.; Jaiswal, A. K. Regulation of Nrf2—an update. *Free Radic. Biol. Med.* **66:**36-44; 2014.

Nogueira, V.; Park, Y.; Chen, C.-C.; Xu, P.-Z.; Chen, M.-L.; Tonic, I.; Unterman, T.; Hay, N. Akt determines replicative senescence and oxidative or oncogenic premature senescence and sensitizes cells to oxidative apoptosis. *Cancer Cell* **14:**458-470; 2008.

Noh YH, Baek JY, Jeong W, Rhee SG, Chang TS. Sulfiredoxin Translocation into Mitochondria Plays a Crucial Role in Reducing Hyperoxidized Peroxiredoxin III. J. Biol. Chem. 284(13):8470-8477; 2009.

Papandreou, I.; Cairns, R. A.; Fontana, L.; Lim, A. L.; Denko, N. C. HIF-1 mediates adaptation

to hypoxia by actively downregulating mitochondrial oxygen consumption. *Cell Metab.* **3:**187-197; 2006.

Parks, S. K., Chiche, J., Pouyssegur, J. Disrupting proton dynamics and energy metabolism for cancer therapy. *Nat. Rev. Cancer* **13:**611-623; 2013.

Peeters, H.; Debeer, P.; Bairoch, A.; Wilquet, V.; Huysmans, C.; Parthoens, E.; Fryns, J. P.; Gewillig, M.; Nakamura, Y.; Niikawa, N.; Van de Ven, W.; Devriendt, K. PA26 is a candidate gene for heterotaxia in humans: identification of a novel PA26-related gene family in human and mouse. *Hum. Genet.* **112:**573-580; 2003.

Petronilli, V.; Penzo, D.; Scorrano, L.; Bernardi, P.; Di Lisa, F. The mitochondrial permeability transition, release of cytochrome c and cell death: Correlation with the duration of pore openings in situ. *J. Biol. Chem.* **276:**12030-12034; 2001.

Popovic, D., Vucic, D., Dikic, I. Ubiquitination in disease pathogenesis and treatment. *Nat. Med.* **11:**1242-1253; 2014.

Qin, R.; Smyrk, T. C.; Reed, N. R.; Schmidt, R. L.; Schnelldorfer, T.; Chari, S. T.; Petersen, G. M.; Tang, A. H. Combining clinicopathological predictors and molecular biomarkers in the oncogenic K-RAS/Ki67/HIF-1α pathway to predict survival in resectable pancreatic cancer. *Br. J. Cancer* **112:**514-522; 2015.

Rhee, S. G.; Chang, T. S.; Bae, Y. S.; Lee, S. R.; Kang, S. W. Cellular regulation by hydrogen peroxide. *J. Am. Soc. Nephrol.* **14:**S211-S215; 2003.

Rolo, A. P.; Palmeira, C. M. Diabetes and mitochondrial function: role of hyperglycemia and oxidative stress. *Toxicol. Appl. Pharmacol.* **212:**167-178; 2006.

Rudich, A.; Kanety, H.; Bashan, N. Adipose stress-sensing kinases: linking obesity to malfunction. *Trends Endocrinol. Metab.* **18:**291-299; 2007.

Sablina, A. A.; Budanov, A. V.; Ilyinskaya, G. V.; Agapova, L. S.; Kravchenko, J. E.; Chumakov,

P. M. The antioxidant function of the p53 tumor suppressor. *Nat. Med.* **11:**1306-1313; 2005.

Sanli, T.; Linher-Melville, K.; Tsakiridis, T.; Singh, G. Sestrin2 modulates AMPK subunit expression and its response to ionizing radiation in breast cancer cells. *PLoS One* **7:**e32035; 2012.

Scholte, H. R. The biochemical basis of mitochondrial diseases. J. Bioenerg. Biomembr. 20:161-191; 1988.

Scorrano, L.; Penzo, D.; Petronilli, V.; Pagano, F.; Bernardi, P. Arachidonic acid causes cell death through the mitochondrial permeability transition: Implications for tumor necrosis factor-α apoptotic signaling. *J. Biol. Chem.* **276:**12035-12040; 2001.

Semenza, G. L. Hypoxia-inducible factor 1 and cancer pathogenesis. *IUBMB Life* **60:**591–597; 2008.

Semenza, G. L. Oxygen sensing, hypoxia-inducible factors, and disease pathophysiology. *Annu. Rev. Pathol.* **9:**47-71; 2014.

Semenza, G. L. Targeting HIF-1 for cancer therapy. *Nat. Rev. Cancer* **3:**721-732; 2003.

Semenza, G. L.; Roth, P. H.; Fang, H. M.; Wang, G. L. Transcriptional regulation of genes encoding glycolytic enzymes by hypoxia-inducible factor 1. *J. Biol. Chem.* **269:**23757-23763; 1994.

Seo, K.; Seo, S.; Han, J. Y.; Ki, S. H.; Shin, S. M. Resveratrol attenuates methylglyoxal-induced mitochondrial dysfunction and apoptosis by Sestrin2 induction. *Toxicol. Appl. Pharmacol.* **280:**314-322; 2014.

Serra, D.; Mera, P.; Malandrino, M. I.; Mir, J. F.; Herrero, L. Mitochondrial fatty acid oxidation in obesity. *Antioxid. Redox Signal.* **19:**269-284; 2012.

Shen, A.; Chen, H.; Chen, Y.; Lin, J.; Lin, W.; Liu, L.; Sferra, T. J.; Peng, J. Pien Tze Huang

Overcomes Multidrug Resistance and Epithelial-Mesenchymal Transition in Human Colorectal Carcinoma Cells via Suppression of TGF-β Pathway. *Evid. Based Complement Alternat. Med.* **2014:**679436; 2014.

Shimojo, Y.; Akimoto, M.; Hisanaga, T.; Tanaka, T.; Tajima, Y.; Honma, Y.; Takenaga, K. Attenuation of reactive oxygen species by antioxidants suppresses hypoxia-induced epithelial-mesenchymal transition and metastasis of pancreatic cancer cells. *Clin. Exp. Metastasis* **30:**143-154; 2013.

Shin, B. Y.; Jin, S. H.; Cho, I. J.; Ki, S. H. Nrf2-ARE pathway regulates induction of Sestrin-2 expression. *Free Radic. Biol. Med.* **53:**834-841; 2012.

Shin, S. M.; Cho, I. J.; Kim, S. G. Resveratrol protects mitochondria against oxidative stress through AMP-activated protein kinase-mediated glycogen synthase kinase-3β inhibition downstream of poly(ADP-ribose)polymerase-LKB1 pathway. *Mol. Pharmacol.* **76:**884-895; 2009.

Shin, S. M.; Kim, S. G. Inhibition of arachidonic acid and iron-induced mitochondrial dysfunction and apoptosis by oltipraz and novel 1,2-dithiole-3-thione congeners. *Mol. Pharmacol.* **75:**242-253; 2009.

Sies, H. Role of metabolic H_2O_2 generation: redox signaling and oxidative stress. *J. Biol. Chem.* **289:**8735-8741; 2014.

Sies, H.; Stahl, W.; Sevanian, A. Nutritional, dietary and postprandial oxidative stress. *J. Nutr.* **135:**969-972; 2005.

Sotgia, F.; Martinez-Outschoorn, U. E.; Lisanti, M. P. Mitochondrial oxidative stress drives tumor progression and metastasis: should we use antioxidants as a key component of cancer treatment and prevention? *BMC Med.* **9:**62; 2011.

Steinberg, G. R.; Kemp, B. E. AMPK in health and disease. *Physiol. Rev*. **89:**1025-1078; 2009.

Su, Y.; Loos, M.; Giese, N.; Metzen, E.; Büchler, M. W.; Friess, H.; Kornberg, A.; Büchler, P. Prolyl hydroxylase-2 (PHD2) exerts tumor-suppressive activity in pancreatic cancer. *Cancer* **118:**960-972; 2012.

Sun, W.; Jelkmann, W.; Depping, R. Prolyl-4-hydroxylase 2 enhances hypoxia-induced glioblastoma cell death by regulating the gene expression of hypoxia-inducible factor-α. *Cell Death Dis.* **5:**e1322; 2014.

Tran, H.; Brunet, A.; Grenier, J. M.; Datta, S. R.; Fornace, A. J.; DiStefano, P. S.; Chiang, L. W.; Greenberg, M. E. DNA repair pathway stimulated by the forkhead transcription factor FOXO3a through the Gadd45 protein. *Science* **296:**530-534; 2002.

Treins, C.; Murdaca, J.; Van Obberghen, E.; Giorgetti-Peraldi, S. AMPKactivation inhibits the expression of HIF-1α induced by insulin and IGF-1. *Biochem. Biophys. Res. Commun.* **342:**1197-1202; 2006.

Valko, M.; Leibfritz, D.; Moncol, J.; Cronin, M. T.; Mazur, M.; Telser, J. Free radicals and antioxidants in normal physiological functions and human disease. *Int. J. Biochem. Cell Biol.* **39:**44-84; 2007.

Valko, M.; Rhodes, C. J.; Moncol, J.; Izakovic, M.; Mazur, M. Free radicals, metals and antioxidants in oxidative stress-induced cancer. *Chem. Biol. Interact.* **160:**1-40; 2006.

Velasco-Miguel, S.; Buckbinder, L.; Jean, P.; Gelbert, L.; Talbott, R.; Laidlaw, J.; Seizinger, B.; Kley, N. PA26, a novel target of the p53 tumor suppressor and member of the GADD family of DNA damage and growth arrest inducible genes. *Oncogene* **18:**127-137; 1999.

Wang, G. L.; Jiang, B. H.; Rue, E. A.; Semenza, G. L. Hypoxia-inducible factor 1 is a basic-helix-loop-helix-PAS heterodimer regulated by cellular O_2 tension. *Proc. Natl. Acad. Sci. USA.* **92:**5510-5514; 1995.

Wang, X. The expanding role of mitochondria in apoptosis. *Gene. Dev.* **15:**2922-2933; 2001.

Waris, G.; Ahsan, H. Reactive oxygen species: role in the development of cancer and various chronic conditions. *J. Carcinog.* **5:**14; 2006.

Warolin, J.; Coenen, K. R.; Kantor, J. L.; Whitaker, L. E.; Wang, L.; Acra, S. A.; Roberts, L. J. 2nd.; Buchowski, M. S. The relationship of oxidative stress, adiposity and metabolic risk factors in healthy Black and White American youth. *Pediatr. Obes.* **9:**43-52; 2014.

Wei, J. L.; Fu, Z. X.; Fang, M.; Guo, J. B.; Zhao, Q. N.; Lu, W. D.; Zhou, Q. Y. Decreased expression of sestrin 2 predicts unfavorable outcome in colorectal cancer. *Oncol. Rep.* **33:**1349-1357; 2015.

Weidemann, A.; Johnson, R. S. Biology of HIF-1α. *Cell Death Differ.* **15:**621-627; 2008.

Wenger, R. H.; Gassmann, M. Oxygen(es) and the hypoxia-inducible factor-1. *Biol. Chem.* **378:**609-616; 1997.

WHO.; UNICEF. Progress on Drinking Water and Sanitation, *UNICEF: New York, WHO Geneva.* 2012.

Xi, J.; Wang, H.; Mueller, R. A.; Norfleet, E. A.; Xu, Z. Mechanism for resveratrol-induced cardioprotection against reperfusion injury involves glycogen synthase kinase 3β and mitochondrial permeability transition pore. *Eur. J. Pharmacol.* **604:**111-116; 2009.

Yang, M. H.; Wu, M. Z.; Chiou, S. H.; Chen, P. M. Chang, S. Y; Liu, C. J.; Teng, S. C.; Wu, K. J. Direct regulation of TWIST by HIF-1alpha promotes metastasis. *Nat. Cell Biol.* **10:**295-305; 2008.

Yang, Y.; Cuevas, S.; Yang, S.; Villar, V. A.; Escano, C.; Asico, L.; Yu, P.; Jiang, X.; Weinman, E. J.; Armando, I.; Jose, P. A. Sestrin2 decreases renal oxidative stress, lowers blood pressure, and mediates dopamine d2 receptor-induced inhibition of reactive oxygen species production. *Hypertension* **64:**825-832; 2014.

Yee Koh, M.; Spivak-Kroizman, T. R.; Powis, G. HIF-1 regulation: not so easy come, easy go.

Trends Biochem. Sci. **33:**526-534; 2008.

Yu, T.; Robotham, J. L.; Yoon, Y. Increased production of reactive oxygen species in hyperglycemic conditions requires dynamic change of mitochondrial morphology. *Proc. Natl. Acad. Sci. USA.* **103:**2653-2658; 2006.

Zoncu, R.; Efeyan, A.; Sabatini, D. M. mTOR: from growth signal integration to cancer, diabetes and ageing. *Nat. Rev. Mol. Cell Biol.* **12:**21-35; 2011.

ABSTRACT

The Role of Sestrin2 in Metabolic Stress

Kyuhwa Seo

Advisor: Prof. Sang Mi Shin, Ph. D.

College of Pharmacy,

Graduate School of Chosun University

Cells require energy to support for their growth and proliferation. Mitochondria are cellular organelles which have energy-producing activity using nutrients and oxygen. Therefore, proper supplement of nutrients and oxygen is important to preserve the mitochondrial function. However, their imbalance leads to ATP depletion, thereby inducing energy metabolic stress. Metabolic stress disturbs the function of mitochondrial electron transport chain and leads to reactive oxygen species (ROS) production. Excessive ROS production causes oxidative stress and triggers signal-transduction pathway that alters gene expression. Therefore, cells have diverse antioxidant systems to preserve cellular redox homeostasis. Sestrin2 (SESN2) as an antioxidant protein is regulated in response to diverse stress including oxidative stress. SESN2 modulates cellular redox homeostasis through the regeneration of peroxiredoxins, therefore contributes to inhibit intracellular ROS. This study investigated the mechanism underlying the role of SESN2 in metabolic stress from deprivation of glucose or oxygen.

The first study demonstrates protective role of SESN2 from the glucose deprivation-induced metabolic stress. First, SESN2 expression was higher in the hepatocytes isolated from

fasted mice than nonfasted mice. Glucose deprivation induced SESN2 expression in hepatocyte-derived cells (AML12, Huh7 and HepG2). However, in HepG2 cell, high glucose (more than normal condition) did not changed SESN2 expression. Glucose deprivation increased mRNA expression and luciferase activity of SESN2. To demonstrate whether glucose deprivation-induced SESN2 induction is accompanied by Nrf2 transactivation, the phosphorylation of Nrf2 was examined. The phosphorylation of Nrf2 was increased by glucose deprivation. To identify the role of SESN2 in glucose deprivation-mediated mitochondrial damage, cells that stably overexpressed SESN2 were prepared. Glucose deprivation decreased the mitochondrial membrane permeability and mitochondrial DNA (mtDNA) content, and increased ADP/ATP ratio. However, SESN2-overexpressed cells decreased the increased ADP/ATP ratio and restored the mitochondrial membrane permeability and mtDNA content under glucose deprivation. Indeed, overexpression of SESN2 protected cells against glucose deprivation-induces apoptosis. The protective effect of SESN2 in mitochondria against glucose deprivation was reversed by siRNA knockdown of SESN2. To understand the cellular signaling underlying the protective activity of SESN2 in glucose deprivation-induced mitochondrial dysfunction and apoptosis, AMP-activated protein kinase (AMPK), a cellular energy sensor, was mutated. The recovery of changes in mitochondria membrane permeability examined under glucose deprivation by SESN2 overexpression was significantly reversed by DN-AMPK-overexpressed cells. Treatment with 5-aminoimidazole-4-carboxamide-1-β-d-ribofuranoside (AICAR), an AMPK activator, protected cell death against glucose deprivation. Finally, these results provide that the role of SESN2 in protection of mitochondrial damage and cell death in glucose deprivation, which is associated in part through AMPK activation.

The second study investigates effect of SESN2 on hypoxia (deprivation of oxygen)-induced altered signaling pathways. Hypoxia-inducible factor-1α (HIF-1α) is an oxygen-

dependent transcription factor, which plays a crucial role in tumor growth by inducing target genes involved in angiogenesis and glycolysis in cancer cells. This study examined that the inhibitory effect of SESN2 on hypoxia-induced HIF-1α accumulation and cancer cell metastasis. First, SESN2 overexpression repressed accumulated HIF-1α level in HEK293 cells. To verify whether SESN2 have inhibitory effect on HIF-1α accumulation in colorectal cancer cells, HCT116 and HT29 cells were incubated with hypoxia or $CoCl_2$ (hypoxia-mimicking agent). Hypoxia or $CoCl_2$ treatment accumulated HIF-1α protein, but infection of adenovirus-SESN2 (Ad-SESN2) decreased hypoxia- or $CoCl_2$-induced HIF-1α accumulation. In addition, Ad-SESN2 diminished $CoCl_2$-induced hypoxia response element (HRE) luciferase activity and mRNA level of HIF-1α-driven genes. To examine the role of SESN2 in HIF-1α-mediated cancer cell adaptive response, *in vitro* cell migration and invasion was observed. Ad-SESN2 infected cells were found to inhibit *in vitro* serum-induced cell migration and invasion. To determine whether SESN2 inhibits HIF-1α in transcriptional step, mRNA level of HIF-1α was examined. The mRNA level of HIF-1α was not affected by Ad-SESN2, suggesting that posttranscriptional mechanism possibly might be involved. To detect time period of HIF-1α protein degradation, cells were treated with cycloheximide (an inhibitor of translation) and $CoCl_2$, the level of HIF-1α protein was examined. As a result, the level of HIF-1α was more decreased in Ad-SESN2 at detect time points. In addition, Ad-SESN2 facilitated ubiquitination of HIF-1α protein. Hydroxyl HIF-1α (OH-HIF-1α) contributes to increasing ubiquitination of HIF-1α. Ad-SESN2 increased OH-HIF-1α level in hypoxia and $CoCl_2$ treatment. To examine possibility whether AMPK was accompanied in suppression of HIF-1α by SESN2, Ad-SESN2 cells were transfected with an siRNA AMPKα. Knockdown of AMPKα abolished Ad-SESN2-mediated increased in OH-HIF-1α and reduced level of HIF-1α. Moreover, DN-AMPK

restored the decreased HIF-1α accumulation by Ad-SESN2. Next, to verify whether increased OH-HIF-1α by SESN2 affect on the cancer cell metastasis, cells were treated with dimethyloxalylglycine (DMOG), an inhibitor of PHD activity. DMOG treatment reversed Ad-SESN2-induced increased in OH-HIF-1α and reduced HIF-1α accumulation. Consistently, DMOG treatment abrogated the inhibitory effect of serum-induced *in vitro* cell migration and invasion in Ad-SESN2. Finally, these results suggest that SESN2 promotes degradation of HIF-1α protein and inhibits *in vitro* cell migration invasion in part from AMPK pathway.

Collectively, this study identified the role of SESN2 in metabolic stress. This study suggests that SESN2 protects metabolic stress-induced mitochondrial impairment and cytotoxicity, and inhibits cancer cell adaptation in hypoxia. Therefore, SESN2 may become a promising therapeutic target of metabolic stress-induced diseases.